



HAL
open science

Pharmacological inhibition of the F₁-ATPase/P2Y₁ pathway suppresses the effect of apolipoprotein A1 on endothelial nitric oxide synthesis and vasorelaxation

Cendrine Cabou, Paula Honorato, Luis Briceño, Lamia Ghezali, Thibaut Duparc, Marcelo León, Guillaume Combes, Laure Frayssinhes, Audren Fournel, Anne Abot, et al.

► To cite this version:

Cendrine Cabou, Paula Honorato, Luis Briceño, Lamia Ghezali, Thibaut Duparc, et al.. Pharmacological inhibition of the F₁-ATPase/P2Y₁ pathway suppresses the effect of apolipoprotein A1 on endothelial nitric oxide synthesis and vasorelaxation. *Acta Physiologica*, 2019, 1 (3), pp.e13268. 10.1111/apha.13268 . inserm-02074732

HAL Id: inserm-02074732

<https://inserm.hal.science/inserm-02074732>

Submitted on 20 Mar 2019

HAL is a multi-disciplinary open access archive for the deposit and dissemination of scientific research documents, whether they are published or not. The documents may come from teaching and research institutions in France or abroad, or from public or private research centers.

L'archive ouverte pluridisciplinaire **HAL**, est destinée au dépôt et à la diffusion de documents scientifiques de niveau recherche, publiés ou non, émanant des établissements d'enseignement et de recherche français ou étrangers, des laboratoires publics ou privés.

Copyright

Pharmacological inhibition of the F₁-ATPase/P2Y₁ pathway suppresses the effect of apolipoprotein A1 on endothelial nitric oxide synthesis and vasorelaxation

Short title: F₁-ATPase/P2Y₁ axis triggers vasorelaxation

Cendrine Cabou^{1,2*}, Paula Honorato^{3*}, Luis Briceño³, Lamia Ghezali¹, Thibaut Duparc¹, Marcelo León³, Guillaume Combes¹, Laure Frayssinhes¹, Audren Fournel⁴, Anne Abot⁴, Bernard Masri¹, Nicol Parada³, Valeria Aguilera³, Claudio Aguayo^{3,5}, Claude Knauf⁴, Marcelo González^{5,6}, Claudia Radojkovic^{3&}, Laurent O. Martinez^{1&}

¹ INSERM, University of Toulouse, Paul Sabatier University, UMR1048, Institute of Metabolic and Cardiovascular Diseases, I2MC, Toulouse, France.

² Department of Human Physiology, Faculty of Pharmacy, University Paul Sabatier, Toulouse, France.

³ Department of Clinical Biochemistry and Immunology, Faculty of Pharmacy, Universidad de Concepción, Concepción, Chile.

⁴ UMR 1220, IRSD, INSERM, INRA, ENVT, University of Toulouse, European Associated Laboratory NeuroMicrobiota (INSERM/UCL), Toulouse, France.

⁵ Group of Research and Innovation in Vascular Health (GRIVAS Health), Chile.

⁶ Vascular Physiology Laboratory, Department of Physiology, Faculty of Biological Sciences, and Department of Obstetrics and Gynecology, Faculty of Medicine, Universidad de Concepción, Concepción, Chile.

Authorship notes:

* C. Cabou and P. Honorato contributed equally to the experimental development of this research.

& L.O. Martinez (Laurent.martinez@inserm.fr) and C. Radojkovic are co-senior authors.

Corresponding author:

C.Radojkovic. Departamento de Bioquímica Clínica e Inmunología, Facultad de Farmacia, Universidad de Concepción. Barrio Universitario s/n, Concepción, Chile. Tel: +56 41 2203451, Email: cradojkovic@udec.cl

Keywords: Apolipoprotein A1, F₁-ATPase, purinergic receptors, endothelial cells, nitric oxide

ABSTRACT

Aim: The contribution of apolipoprotein A1 (APOA1), the major apolipoprotein of high-density lipoprotein (HDL), to endothelium-dependent vasodilatation is unclear, and there is little information regarding endothelial receptors involved in this effect. Ecto-F₁-ATPase is a receptor for APOA1, and its activity in endothelial cells is coupled to adenosine diphosphate (ADP)-sensitive P2Y receptors (P2Y ADP receptors). Ecto-F₁-ATPase is involved in APOA1-mediated cell proliferation and HDL transcytosis. Here we investigated the effect of lipid-free APOA1 and the involvement of ecto-F₁-ATPase and P2Y ADP receptors on nitric oxide (NO) synthesis and the regulation of vascular tone.

Method: NO synthesis was assessed in human endothelial cells from umbilical veins (HUVECs) and isolated mouse aortas. Changes in vascular tone were evaluated by isometric force measurements in isolated human umbilical and placental veins and by assessing femoral artery blood flow in conscious mice.

Results: Physiological concentrations of lipid-free APOA1 enhanced endothelial NO synthesis, which was abolished by inhibitors of endothelial nitric oxide synthase (eNOS) and of the ecto-F₁-ATPase/P2Y₁ axis. Accordingly, APOA1 inhibited vasoconstriction induced by thromboxane A2 receptor agonist and increased femoral artery blood flow in mice. These effects were blunted by inhibitors of eNOS, ecto-F₁-ATPase and P2Y₁ receptor.

Conclusions: Using a pharmacological approach, we thus found that APOA1 promotes endothelial NO production and thereby controls vascular tone in a process that requires activation of the ecto-F₁-ATPase/P2Y₁ pathway by APOA1. Pharmacological targeting of this pathway with respect to vascular diseases should be explored.

1 - INTRODUCTION

Endothelial dysfunction is common to all cardiovascular diseases. It is characterized by a shift in the actions of the endothelium toward a proinflammatory state, prothrombotic properties and reduced vasorelaxation. Numerous cardiovascular risk factors are associated with altered endothelium-dependent relaxation, such as smoking, hypertension, dyslipidemia and diabetes ¹.

At the interface with components of the blood, the endothelium senses chemical or mechanical (shear stress) changes in the blood. In response to these *stimuli*, the endothelium secretes vasoactive factors to regulate vascular tone and flow. Endothelium-derived nitric oxide (NO) plays a key role in this process by producing direct effects at the vascular wall. In particular, NO promotes vasorelaxation by acting on vascular smooth muscle cells, inhibits platelet activation and decreases adhesion molecule expression and leukocyte extravasation, reducing the inflammatory response involved in atherosclerotic plaque development ^{1,2}. Therefore, disturbance of NO production or bioavailability, as measured indirectly by an impairment of the vasodilatory response, is considered a predictive factor for the development of cardiovascular diseases ^{1,2}. In endothelial cells, NO is produced by the conversion of L-arginine to L-citrulline by the enzymatic action of the endothelial isoform of nitric oxide synthase (eNOS). Reduced NO bioavailability, commonly observed in individuals with cardiovascular risk factors, is associated with an increased risk of adverse cardiovascular events ^{1,2}. Thus, factors that improve endothelial NO bioavailability are important for preserving vascular homeostasis.

High-density lipoprotein (HDL) stimulates eNOS-mediated NO production *in vitro* and *in vivo* ³⁻⁸. Moreover, in dyslipidemic patients, the infusion of reconstituted HDL particles containing apolipoprotein A1 (APOA1) and phosphatidylcholine restores endothelium-dependent vasodilatation by increasing NO bioavailability ^{9,10}. Different HDL receptors have been identified on endothelial cells from different vascular beds, but it has not yet been clarified how they each contribute to endothelial function and vascular homeostasis. HDL binding to scavenger receptor class B type I (SR-BI) increases eNOS activity and NO-dependent vasodilatation of the aorta through a process that requires APOA1 in HDL particles ¹¹. Activation of eNOS also occurs through receptors sensitive to components transported by HDL, including sphingolipids (such as ceramide ¹² and sphingosine-1-phosphate ⁶), estrogen ¹³ and paraoxonase ¹⁷. APOA1 is the main apolipoprotein of HDL, and its lipid-free or lipid-poor form accounts for ~5–10% of total APOA1 in human plasma ¹⁴⁻¹⁷. In bovine aortic endothelial cells, both lipid-free APOA1 and HDL enhance eNOS phosphorylation,

and this effect correlates with NO synthesis ¹⁸. In addition, APOA1 alone increases eNOS protein half-life in human vascular endothelial cells through the activation of protein kinase B (PKB/Akt) and mitogen-activated protein kinase (MAPK) pathways ³. In hypercholesterolemic low-density lipoprotein (LDL) receptor–knockout mice, oral administration of an APOA1 mimetic peptide, D-4F, improves endothelium-dependent vasodilatation and reduces the thickness of the arterial wall ¹⁹. However, there is little information regarding the receptors that would be involved in such effects triggered by lipid-free APOA1.

Ecto-F₁-ATPase is an APOA1 receptor expressed on the surface of different cell types, including hepatocytes and endothelial cells ²⁰⁻²³. APOA1 binding to ecto-F₁-ATPase stimulates its ATPase activity, which generates extracellular adenosine diphosphate (ADP), a process that is prevented by the F₁-ATPase inhibitor Inhibitory Factor 1 (IF1) ²⁰⁻²³. This newly generated extracellular ADP binds to purinergic ADP-sensitive P2Y receptors (P2Y ADP receptors). Depending on the cell type, distinct P2Y receptors are activated, which translates into distinct cellular processes. For example, on hepatocytes, ecto-F₁-ATPase activity is coupled to the P2Y₁₃ receptor and contributes to HDL holoparticle endocytosis and hepato-biliary reverse cholesterol transport *in vivo* ²⁴⁻²⁶. In human umbilical veins endothelial cells (HUVECs) and in endothelial progenitor cells, ecto-F₁-ATPase activation by APOA1 stimulates endothelial cell survival and proliferation ^{21,23}. A new study has demonstrated that these effects on endothelial cells occur through the specific activation of the P2Y₁ receptor and involve the phosphatidylinositol-3-kinase β (PI3K β)/Akt survival signaling pathway ²⁷. It is of interest that several purinergic receptors expressed on endothelial cells have been reported to contribute to NO-dependent vasorelaxation, including P2Y₁ (ADP), P2Y₂ (ATP, UTP), P2Y₆ (UDP) and P2X₄ (ATP) ²⁸⁻³³.

Thus, because HDL/APOA1 and purinergic receptors are clearly of fundamental importance in NO-mediated endothelium vasorelaxation, we investigated the involvement of ecto-F₁-ATPase and ADP-sensitive P2 receptors in APOA1-mediated NO synthesis and in the regulation of vascular tone. For this investigation, we used HUVECs and human and mouse blood vessels, and we measured arterial blood flow in conscious mice.

2 - RESULTS

2.1 - APOA1 increases eNOS activity and NO production in human endothelial cells and mouse aortas.

To investigate whether APOA1 directly stimulates eNOS activity, we measured the production of L-[³H]-citrulline from L-[³H]-arginine in HUVECs exposed to lipid-free APOA1 purified from human plasma. The basal eNOS activity over a 30-min period was 0.112 ± 0.005 pmol of L-[³H]-citrulline produced $\cdot \mu\text{g}$ of cellular protein⁻¹ (data not shown). Exposure to APOA1 for 30 min increased eNOS activity in a dose-dependent manner, with a maximal ~1.5-fold increase occurring at $50 \mu\text{g} \cdot \text{mL}^{-1}$ APOA1 (corresponding to $1.8 \mu\text{mol} \cdot \text{L}^{-1}$), which was similar to eNOS activity elicited by $1 \text{mmol} \cdot \text{L}^{-1}$ histamine (Figure 1A). Pre-incubation of endothelial cells with the NOS inhibitor L-N^G-nitroarginine methyl ester (L-NAME, $100 \text{nmol} \cdot \text{L}^{-1}$) fully abolished APOA1-induced eNOS activity (Figure 1B). We further assessed whether APOA1 directly influenced NO production in endothelial cells by using the NO-sensitive fluorescence probe DAF-FM-DA. APOA1 ($50 \mu\text{g} \cdot \text{mL}^{-1}$) stimulated NO production within 5 min of its addition, and this effect was maintained over the 30-min time period (Figure 1C) and was blocked by L-NAME (Figure 1D). As a control, lipid-free APOA2 ($50 \mu\text{g} \cdot \text{mL}^{-1}$), another HDL protein, did not induce NO production (Figure 1D). APOA1 treatment in HUVECs ($50 \mu\text{g} \cdot \text{mL}^{-1}$) also stimulated eNOS phosphorylation at serine 1177 (p-Ser¹¹⁷⁷), a post-translational modification associated with higher eNOS activity³⁴, in a time-dependent manner, with maximal phosphorylation occurring within 15–20 min (Figure 2A). We further evaluated the effect of APOA1 on NO production *ex-vivo* in mouse aortas using a NO-specific amperometric probe. We observed that APOA1 increased aortic NO production in a dose-dependent manner, with a significant effect after a 1-min incubation that remained significant throughout the studied period (Figure 1E). In the same set of experiments, pharmacological blockade of NOS by addition of L-N^G-monomethyl arginine (L-NMMA, $500 \mu\text{mol} \cdot \text{L}^{-1}$) in the medium together with APOA1 ($50 \mu\text{g} \cdot \text{mL}^{-1}$) completely inhibited APOA1-induced NO production (Figure 1F). In the same aortic segments, immunostaining with an antibody against p-Ser¹¹⁷⁷-eNOS revealed that exposure to $50 \mu\text{g} \cdot \text{mL}^{-1}$ APOA1 increased eNOS phosphorylation in the endothelial lining relative to that in the presence of phosphate-buffered saline (PBS; Figure 2C, APOA1 vs. PBS panels).

Taken together, these data demonstrate that APOA1 induces NO synthesis by increasing eNOS activity.

2.2 - APOA1-induced eNOS activity and endothelial NO production occurs through ecto-F₁-ATPase.

Ecto-F₁-ATPase is an APOA1 receptor that is expressed in endothelial cells and involved in APOA1-mediated endothelial cell survival, as stimulation of its activity by APOA1 inhibits endothelial cell apoptosis and promotes proliferation^{21,27}. We thus assessed whether ecto-F₁-ATPase was also involved in APOA1-induced NO synthesis. First, the effects of APOA1 exposure ($50 \mu\text{g} \cdot \text{mL}^{-1}$, equivalent to $1.8 \mu\text{mol} \cdot \text{L}^{-1}$) on eNOS activity and NO production in HUVECs were totally abolished when cells were pre-treated with IF1 ($1.8 \mu\text{mol} \cdot \text{mL}^{-1}$) or Oligomycin ($125 \text{nmol} \cdot \text{L}^{-1}$), two specific inhibitors of F₁-ATPase activity^{27,35,36} (Figures 3A-B). Accordingly, APOA1-mediated eNOS phosphorylation at Ser¹¹⁷⁷ was repressed when ecto-F₁-ATPase activity was inhibited with IF1 (Figure 2B). We then measured the effect of IF1 on NO production in aortas *ex vivo* exposed to $50 \mu\text{g} \cdot \text{mL}^{-1}$ APOA1 and found that IF1 ($3.6 \mu\text{mol} \cdot \text{L}^{-1}$) dramatically inhibited the stimulatory action of APOA1 on NO production (Figure 3C). Furthermore, immunohistochemical analyses of mouse aortic segments showed that APOA1-induced eNOS phosphorylation at Ser¹¹⁷⁷ was inhibited when the aortas were pre-treated with the F₁-ATPase inhibitor IF1 (Figure 2C, APOA1+IF1 vs APOA1). We further examined the possible contributions of two other APOA1-sensitive receptors to NO synthesis, *i.e.*, ATP binding cassette A1 (ABCA1) and SR-BI. Previously, we demonstrated that neither ABCA1 nor SR-BI is involved in the proliferative and pro-survival effects of APOA1 on endothelial cells that are solely mediated by ecto-F₁-ATPase activation²¹. In agreement with these observations, the effect of APOA1 on eNOS activity was fully maintained under treatment with neutralizing antibodies directed against ABCA1³⁷ and SR-BI³⁸ (Figure 3D-E), indicating that neither of these receptors was involved in the increased of eNOS activity induced by APOA1. Interestingly, the effect of HDL on eNOS activity was slightly, but not significantly, higher than that for APOA1 ($p = 0.09$) but was inhibited by SR-BI antibody (Figure 3E). This is in line with a previous study that has shown that the lipid moiety associated with APOA1 within HDL particles is essential for the interaction with SR-BI to activate eNOS¹¹. Taken together, these data imply that, in primary human endothelial cells and mouse aortas, APOA1 stimulates NO synthesis by activating ecto-F₁-ATPase.

2.3 - P2Y₁ receptor mediates eNOS activity and endothelial NO production in response to APOA1 stimulation.

On endothelial cells, APOA1 binding to ecto-F₁-ATPase stimulates its ATPase activity and generates extracellular ADP^{21,22}. We thus investigated whether extracellular ADP generated from stimulation of ecto-F₁-ATPase by APOA1 activates an ADP-sensitive P2Y receptor on these cells.

Among purinergic receptors sensitive to ADP, endothelial cells predominantly express P2Y₁ receptor^{39,40}. Accordingly, P2Y₁ protein was found to be expressed in HUVEC, but P2Y₁₂ was not or barely detectable (Figure 4A), whereas both P2Y₁ and P2Y₁₂ ADP-receptors were highly expressed in human platelets, as reported⁴¹. It has been shown that both P2Y₁ and P2Y₁₂ receptors are N-glycosylated⁴², which supports that we have them both detected at ~55 kDa (Figure 4A), a higher molecular weight than the one calculated from their amino-acid sequence. Previous studies have described that multiple bands observed for P2Y₁ are probably the effect of protein glycosylation and were shown to disappear after total receptor deglycosylation⁴³. Thus, the minor bands observed in platelet and HUVECs could be attributed to different levels of P2Y₁ glycosylation (Figure 4A, upper panel). Regarding P2Y₁₂, we and others have previously reported that P2Y₁₂ mRNA was barely detectable in HUVECs^{27,40}, which supports that the protein was not detected (Figure 4A, lower panel) and exclude that a glycosylation difference between platelets and HUVECs would affect antibody reactivity for P2Y₁₂ detection in HUVECs. We thus investigated whether the P2Y₁ receptor was involved in NO synthesis induced by APOA1. As reported^{30,32,44-46}, we first observed that treatment of HUVECs with ADP increased eNOS activity in a concentration-dependent manner with maximal activation obtained at 10 μmol • L⁻¹ (Figure 4B). In another set of experiments, HUVECs were pre-incubated with either the P2Y₁ inhibitor 2'-deoxy-N⁶-methyladenosine 3',5'-bisphosphate (MRS2179, 10 μmol • L⁻¹) or the P2Y₁₂ inhibitor cangrelor (AR-C69931, 10 μmol • L⁻¹), followed by stimulation with APOA1 (50 μg • mL⁻¹). MRS2179 totally blocked APOA1-induced eNOS activity and NO production in HUVECs, whereas no effect was observed with cangrelor (Figure 4C-D). In line with these observations, treating mouse aortas with 50 μmol • L⁻¹ MRS2179 completely abolished NO production induced by APOA1, whereas this effect was maintained with 50 μmol • L⁻¹ cangrelor (Figure 4E). Taken together, these results reveal a potent contribution of the P2Y₁ receptor, but not of P2Y₁₂, in APOA1-induced endothelial NO synthesis.

2.4 - APOA1 increases endothelial NO-dependent vasodilatation and blood flow through the ecto-F₁-ATPase/P2Y₁ pathway.

The physiological effect of APOA1 on endothelial NO synthesis was evaluated by studying the impact of APOA1 on human vessel reactivity. First, the effect of APOA1 on vascular tone was assessed in small resistance vessel rings isolated from human umbilical and placental veins, which were pre-treated for 15 min with a thromboxane A₂ receptor agonist (U46619, 100 nmol • L⁻¹) to induce smooth muscle cell contraction. This model induces sub-threshold

constrictions and permits to study endothelium-dependent vasodilator response⁴⁷⁻⁴⁹. As expected, incubation of vessel rings with U46619 induced a vasoconstriction of ~ 50% the maximal response to KCl in umbilical veins and ~ 65% in chorionic veins (not shown). Following this 15-min period allowing vessels pre-contraction, time was set at 0 and vasoconstriction at 100%, and APOA1 or PBS (vehicle) was added to the medium containing U46619. As observed in Figure 5A-B, vessels only treated with U46619 (represented by the PBS condition) continued to contract in time to reach a maximum contraction of ~ 150% in umbilical veins and ~ 130% in placental veins. Conversely, exposure to 50 μg • mL⁻¹ APOA1 reduced significantly the progressive contraction induced to U46619, maintaining tension values at ~ 100% throughout the studied period (Figure 5A-B, bar graphs). This response to APOA1 was inhibited by treatment with the NOS inhibitor (L-NAME, 200 μmol • L⁻¹) or when the endothelium was mechanically removed from vessel rings (Figure 5A-B), suggesting that APOA1-mediated vasodilatation depends on endothelial NO production.

We then analyzed the effect of APOA1 on arterial blood flow in awake mice. Systemic infusion of human APOA1 for 45 min increased femoral arterial blood flow in a time- and dose-dependent manner (Figure 6A), and this effect was significant over the recorded period (Figure 6A, bar graph). Arterial blood flow increased by 45–50% with the highest human APOA1 dose (30 nmol • kg⁻¹ • min⁻¹, Figure 6A). In line with these results, systemic infusion of APOA1 increased heart rate by ~ 10 %, and this effect was significant for the highest dose 30 nmol • kg⁻¹ • min⁻¹ over the recorded period (Figure 7A), suggesting the activation of a compensatory mechanism in response to the diminished peripheral resistance. NOS inhibition by L-NMMA fully abolished the blood flow response to systemic APOA1 (Figure 6B) without modifying the mean heart rate (Figure 7B), indicating that this effect depends on the observed action of APOA1 on endothelial NO production. At end of the infusion period with 30 nmol APOA1 • kg⁻¹ • min⁻¹ (t = 45 min), plasma concentration of human APOA1 was 0.52 ± 0.01 mg • mL⁻¹. Interestingly, plasma HDL-C, measured by enzymatic colorimetric method was unchanged (0.56 mg • mL⁻¹ and 0.57 mg • mL⁻¹ at t = 0 and t = 45 min, respectively), indicating that APOA1 infusion for this period of time does not generate HDL particles. Taken together, these results are evidence of a physiological effect of APOA1 on endothelial NO-dependent vasorelaxation and regulation of blood flow.

We next explored through pharmacological approaches whether the ecto-F₁-ATPase/P2Y₁ pathway is involved in endothelium-dependent NO-mediated relaxation in response to APOA1. We first observed that the ecto-F₁-ATPase inhibitor IF1 (1.8 μmol • L⁻¹) abolished the relaxation induced by 50 μg • mL⁻¹ APOA1 on pre-contracted human

umbilical and placental veins (Figure 5C-D). Similarly, the increased blood flow observed in wild-type mice infused with APOA1 was absent when animals were co-infused with IF1 (Figure 6C), and the higher heart rate induced by APOA1 was reduced with IF1 treatment (Figure 7C). In addition, the infusion of an analog of ADP, 2-methylthio-adenosine-5'-diphosphate (2meSADP, $0.7 \mu\text{mol} \cdot \text{kg}^{-1} \cdot \text{min}^{-1}$), significantly increased the mean arterial blood flow by 40% and this effect was blunted in mice receiving L-NMMA (Figure 8A). These data demonstrate that ADP induces endothelial NO-mediated vasodilatation of the femoral artery in mice. Furthermore, inhibition of P2Y₁ receptor with MRS2179 prevented any increase in blood flow induced by 2meSADP (Figure 8B), demonstrating the central role of P2Y₁ in vessel relaxation in response to ADP stimulation. Finally, we evaluated the involvement of the P2Y₁ receptor in the vasodilatory response induced by APOA1 in conscious mice. Intravenous infusion of MRS2179 completely abolished the effect of APOA1 on the arterial blood flow (Figure 8C) and on the heart rate (Figure 7D).

3 - DISCUSSION

This study shows that APOA1 enhances endothelial NO synthesis through an increase in eNOS activity, an effect that promotes the vasodilatory response of human blood vessels *ex vivo* and increases arterial blood flow *in vivo* in conscious mice. In addition, we provide evidence that APOA1 triggers these effects through ecto-F₁-ATPase activity coupled to the activation of the P2Y₁ ADP receptor, which belongs to the family of P2Y purinergic G protein-coupled receptors stimulated by extracellular nucleotides.

Ecto-F₁-ATPase is a cell surface enzymatic complex related to mitochondrial F₁F₀-ATP synthase²⁴. Pioneering studies on hepatocytes demonstrated that the β -chain of ecto-F₁-ATPase is a high-affinity receptor for APOA1 that contributes to endocytosis of whole HDL particles²⁰. Briefly, APOA1 binding to ecto-F₁-ATPase stimulates its ATPase activity, generating extracellular ADP that specifically activates hepatic P2Y₁₃ receptor⁵⁰. This then induces a signaling pathway that activates the small G-protein RhoA and the downstream-located Rho-associated protein kinase I and ultimately leads to actin cytoskeleton reorganization necessary for subsequent clathrin-dependent HDL endocytosis⁵¹. P2Y₁₃-knockout mice display impaired hepatobiliary lipid secretions and are prone to atherosclerosis on an apoE-knockout background^{25,52,53}. As in hepatocytes, APOA1 stimulates the hydrolytic activity of ecto-F₁-ATPase expressed on endothelial cells, generating extracellular ADP^{21,22}. Among P2Y receptors that are preferentially activated by ADP, endothelial cells predominantly express P2Y₁ and, to a

lesser extent, P2Y₁₂ receptors^{22,27,30,40,44}. Consequently, the signal transduction downstream of ecto-F₁-ATPase activation by APOA1 and subsequent cellular processes are different than those in hepatocytes. Hitherto, it has been reported that one of these processes is P2Y₁₂-mediated HDL transcytosis through endothelial cells²². The other is a pro-survival pathway that specifically depends on the P2Y₁ receptor and involves the p110 β PI3K class I isoform (PI3K β) to promote endothelial cell proliferation²⁷. Hence, within a common framework involving the sequential activation of ecto-F₁-ATPase by APOA1, production of extracellular ADP and downstream activation of P2Y-mediated signaling pathways, distinct P2Y receptors can be activated depending on cell type, thus inducing distinct metabolic or vascular events²⁴. The present study demonstrating the functional association between ecto-F₁-ATPase and P2Y₁ in mediating the NO-dependent vasodilator response triggered by APOA1, confirms the central beneficial role of this F₁-ATPase/P2Y axis for the important metabolic and vascular functions of APOA1.

The involvement of P2Y₁ receptor, rather than P2Y₁₂, is consistent with studies on endothelial cells and isolated arteries indicating that P2Y₁ is involved in ADP-mediated eNOS activation and ADP-induced vasodilatation *via* an endothelium/NO-dependent mechanism^{30,32,44-46}. Among other purinergic receptors expressed on endothelial cells, P2X₄ (calcium channel) and P2Y₂ (G_q/G₁₁-coupled receptor) are involved in the control of flow-induced endothelial NO production and vascular tone^{29,33}. Both P2X₄ and P2Y₂ are preferentially activated by extracellular ATP, which can be released in large amounts (*i.e.*, in the micromolar range) in the vascular compartment, from erythrocytes and endothelial cells, particularly under hypoxia or in response to shear stress^{54,55}. Mechanistically, it has been proposed that ATP release induced by shear stress activates P2X₄/P2Y₂ and subsequent Ca²⁺-dependent activation of eNOS^{29,33}. At this stage, how endothelial purinergic receptors interact with one another (or the respective contributions of individual endothelial purinergic receptors) in the control of vascular tone remains elusive. One might hypothesize that the extracellular ADP, resulting from extracellular ATP hydrolysis by ecto-F₁-ATPase under the control of APOA1, which activates P2Y₁-dependent NO production, amplifies or sustains the action of ATP-sensitive purinergic receptors in eNOS activation.

Our analysis of femoral artery blood flow in awake mice supports the physiological relevance of the ecto-F₁-ATPase/P2Y₁ pathway in regulating endothelial NO production and vascular tone. Although we have not investigated whether this pathway is sensitive to flow pattern, other studies have suggested that this is likely. For instance, endothelial cells subjected to an oscillatory flow, a

condition that takes place in atheroprone areas, have higher expression of ecto-F₁-ATPase⁵⁶. Also, another study has recently reported that shear stress-induced endothelial NO production sequentially involves autophagy-mediated endothelial glycolysis, ATP production and release and P2Y₁ signaling⁵⁷.

The P2Y₁ receptor in platelets is involved in platelet shape change and aggregation, and a number of pharmacological agents have been developed as platelet P2Y₁ antagonists⁵⁸. As far as we are aware, there have been no clinical studies evaluating the use of P2Y₁ antagonists as antithrombotic agents in human subjects, but, given the beneficial role of the P2Y₁ receptor in preserving endothelial functions, their clinical potential is questionable.

The identity of intracellular signaling pathway(s) linking P2Y₁ activation to APOA1-mediated NO production has not been addressed in this work, but some hypotheses can be considered. In the present study, we observed that ecto-F₁-ATPase activation by APOA1 in human endothelial cell and mouse aorta stimulated eNOS phosphorylation at serine 1177, which is catalyzed by a number of distinct kinases including Akt, protein kinase A, AMP-activated protein kinase, calcium/calmodulin-dependent protein kinase type II and checkpoint kinase I⁵⁹. APOA1 induces a PI3K β /Akt-dependent signaling pathway to promote endothelial cell proliferation in a process that strictly depends on upstream activation of the ecto-F₁-ATPase/P2Y₁ axis²⁷. Moreover, PI3K β mediates NO production in endothelial cells following the activation of different receptors^{60,61}. Thus, the PI3K β /Akt signaling pathway could be involved in NO production mediated by the APOA1/ecto-F₁-ATPase/P2Y₁ axis. Alternatively, it has been reported that coupling of the P2Y₁ receptor to Gq proteins induces eNOS activation through combined Ca²⁺-dependent conformational modification, as well as PKC δ -dependent phosphorylation of eNOS^{44,57}.

Many different components of HDL activate distinct cell surface receptors and induce endothelial NO-dependent vasorelaxation through different mechanisms⁶². For instance, HDL binding to SR-BI activates eNOS in a process that depends on HDL components in addition to APOA1¹¹. ATP binding cassette G1 and HDL maintain active eNOS dimer levels by promoting efflux of cholesterol and 7-oxysterols⁶³. Also, HDL-associated sphingolipids, such as sphingosin-1-phosphate, cause eNOS-dependent relaxation of pre-contracted aortic rings from mice by binding to the lysophospholipid receptor S1P₃ expressed on endothelial cells⁶. In addition, the HDL-associated enzyme paraoxonase 1 participates in the ability of HDL to stimulate endothelial NO production⁷. In the present study, we bypassed these pathways by using lipid-free APOA1, which remains lipid-free or is poorly lipidated within the first hour of incubation with cells⁶⁴. Furthermore, APOA1-mediated eNOS activity was

totally inhibited by the F₁-ATPase inhibitor IF1, whereas inhibition of ABCA1, another lipid-free APOA1 receptor^{21,65}, and SR-BI, had no effect. We also observed that NO synthesis and the vasodilator effect induced by APOA1 were entirely inhibited by IF1, confirming that the effect of lipid-free APOA1 on NO-mediated vasorelaxation solely depends on ecto-F₁-ATPase. Ecto-F₁-ATPase represents ~70% of the lipid-free APOA1 binding sites on endothelial cells, whereas ABCA1 accounts for the remaining 30%²¹. Thus, whereas endothelial ABCA1 is involved in other processes mediated by APOA1, such as cellular cholesterol efflux⁶⁶ and APOA1 transcytosis⁶⁷, our study indicates that ecto-F₁-ATPase is the sole receptor involved in NO production by endothelial cells and NO-dependent vessel relaxation induced by lipid-free APOA1.

In humans, pre β 1-HDL is mainly lipid-free APOA1⁶⁸ and represents ~5–10% of the total plasma APOA1 concentration^{14,17,69,70}, which equals a plasma concentration in healthy individuals in the range of 50–200 $\mu\text{g} \cdot \text{mL}^{-1}$. In our experiments measuring blood flow in mice, human APOA1 concentration reached at the end of the infusion period was thus slightly above this range, indicating that therapeutic intervention aiming to increase plasma level of functional APOA1 might have some beneficial effect on the vascular tone. Physiologically, one part of the pre β 1-HDL pool is directly released into the circulation after its synthesis in the liver and intestine, and the other part is derived from lipolysis of triglyceride-rich HDL and the interconversion of HDL subclasses by lipid transfer proteins and lipoprotein lipases^{14,17,68}. Hence, these metabolic processes that release substantial quantities of lipid-free APOA1 to the bloodstream may contribute to endothelial function, in addition to the effects produced by APOA1 associated with mature spheroidal HDL. Increasing functional level of lipid-free APOA1 through APOA1 infusion might be challenging in coronary artery disease (CAD) patients for which APOA1 is subject to detrimental modifications such as oxidation or nitration that make it dysfunctional for some of its atheroprotective properties such as its ability to promote cholesterol efflux^{71–73}. Although not investigated yet, it is likely that such APOA1 modifications would also reduce its ability to stimulate ecto-F₁-ATPase.

Other studies support a positive action of lipid-free APOA1 on NO production, eNOS phosphorylation and eNOS protein half-life^{3,18}. In the present study, acute incubation with lipid-free APOA1 increased NO synthesis in primary cultures of human endothelial cells and in aortas isolated from wild-type mice and produced the relaxation of human and mouse blood vessels. Because NO has a very short half-life, these results suggest that APOA1 continuously stimulates the NO synthesis responsible for the observed effects.

Endothelial cells from different blood beds show morphological and functional differences^{74,75}. In this study,

ex vivo vascular reactivity experiments were performed with human veins obtained from umbilical cords and placenta, which correspond to small resistance vessels from the macro and microvascular system, respectively, of the fetoplacental unit^{74,75}. In both vessel types, we observed the vasodilator effect of APOA1 through ecto-F₁-ATPase activity, which was more evident in umbilical veins than in placental veins. Of interest, the vasodilator action of APOA1 was no longer detected in vessels treated with L-NAME or after endothelium removal, suggesting that APOA1-mediated vessel relaxation requires NO synthesis. In these experiments, controls with L-NAME alone and endothelium removal alone have not been performed, which would have unequivocally confirmed the implication of NO production in the effect produced by APOA1. However, it has been reported that endothelium removal does not change the vasoconstrictor response produced by U46619⁷⁶, which is in line with the endothelium-independent vasoconstrictor mechanism described for U46619 that only depends on smooth muscle cells contraction⁷⁷. Accordingly, as mentioned in our experimental settings, endothelium removal or pre-incubation with L-NAME during the pre-contraction period (before APOA1 addition) did not change the percentage of basal pre-contraction obtained with U46619, indicating that, in our conditions, the inhibition of NO production did not increase vascular contractility over the effect of U46619, suggesting that NO was barely synthesized at resting conditions. In vessels exposed to L-NAME or after endothelium removal, APOA1 produced higher isometric tension values than the control (PBS, *i.e.* vessels pre-contracted with U46619) (Figure 5). This observation suggests the presence of other receptors for APOA1 on smooth muscle cells that could trigger vessel constriction. For instance, human smooth muscle cells express high levels of ATP binding cassette A-I (ABCA1)⁷⁸. In endothelial cells, we demonstrated that this receptor is not involved in NO synthesis produced by APOA1, but its contribution in the regulation of smooth muscle contraction has not been assessed yet.

As a limitation of our study, we have not evaluated the implication of P2Y₁ in human vein reactivity experiments. However, our experiments on isolated mouse aortas and *in vivo* measurement of femoral arterial blood flow in mice support that the APOA1/ecto-F₁-ATPase/P2Y₁ axis promote NO synthesis and the vasodilator response, demonstrating the physiological relevance of this pathway. In addition, studies measuring isometric tension in isolated blood vessels from rats and humans demonstrated the vasodilator effect of ADP and its dependence on NO synthesis through the activation of P2Y₁ receptor^{30,79}.

In conclusion, our results support a beneficial action of lipid-free APOA1 with respect to endothelial function. In addition,

our results demonstrate for the first time the pivotal role of the ecto-F₁-ATPase/P2Y₁ pathway in the NO-dependent vasodilator effect that is exerted by APOA1. This new mechanism is of great interest for the development of therapeutic strategies to reduce the pathogenesis of cardiovascular disease.

4. MATERIALS AND METHODS

4.1 - Materials. Collagenase type I from *Clostridium histolyticum* and M-199 medium were purchased from Gibco, Life Technologies (USA). Endothelial Cell Growth Medium-2 BulletKit (EGM-2) was purchased from Clonetics, Lonza (Walkersville, MD, USA). 4-Amino-5-methylamino-2',7'-difluorofluorescein diacetate (DAF-FM-DA) probe, L-N^G-nitroarginine methyl ester (L-NAME) and Pierce BCA Protein Assay Kit were from Thermo Fisher Scientific, Inc. (Waltham, MA, USA). MRS2179 and U46619 were supplied by Tocris Bioscience (Bristol, UK). L-[³H]-arginine was from Perkin Elmer, (Waltham, MA, USA). L-N^G-monomethyl arginine citrate (L-NMMA) was purchased from Abcam, (Cambridge, UK). L-Arginine, adenosine diphosphate (ADP), 2-methylthio-adenosine-5'-diphosphate (2meSADP), cangrelor (AR-C69931MX), oligomycin, Sephadex G-150 and cation ion-exchange resin Dowex 50W were purchased from Sigma-Aldrich (San Luis, MO, USA). Stock solutions of all agonists and antagonists were prepared in distilled water, frozen, thawed on experiment days, and diluted to appropriate working concentrations in phosphate-buffered saline buffer (PBS, pH 7.4). Neutralizing polyclonal antibodies directed against ABCA1 and SR-BI (#NB400-105 and #NB400-113, respectively) were purchased from Novus Biologicals LLC (Littleton, CO, USA).

4.2 - Ethics statement. This study conformed to the principles outlined in the Declaration of Helsinki and received approval from the Ethics Committee of the Universidad de Concepción (Chile), the Ethics Committee of Servicio de Salud Concepción (Chile) and the Comisión Nacional de Investigación Científica y Tecnológica (CONICYT, Chile). Volunteers who agreed to take part in this study signed a written, informed consent form before blood sample or tissue collection.

4.3 - Animals. All procedures involving experimental animals were performed in accordance with the principles and guidelines established by the National Institute of Medical Research (INSERM) and were approved by the local Animal Care and Use Committee. All animals used were male C57BL/6J mice (Janvier Labs, Paris, France). Mice were caged in animal rooms with a light/dark schedule of 12 h/12 h and were fed *ad libitum* with a normal mouse chow (#R04-10,

SAFE, Epinay-sur-Orge, France; content: 59.9% carbohydrate, 16.1% protein, 3.1% fat).

4.4 - Cell culture. HUVECs (Lonza) were seeded on gelatin-covered dishes in growth medium (M-199 medium supplemented with EGM-2 BulletKit) and incubated at 37°C and 5% CO₂ until 80–90% confluent. Cells were recovered using a 0.1% trypsin/EDTA solution. For experiments, HUVECs were used between the first and sixth passages.

4.5 - Human APOA1 and APOA2 isolation. Plasma samples were obtained from young, healthy donors (20–28 years old), who had not eaten for 10 h before we took the samples. HDL was isolated from pooled plasma by sequential ultracentrifugation⁸⁰. HDL was delipidated with a chloroform/methanol mixture⁸¹, and APOA1 and APOA2 were isolated by ion exchange chromatography on HiTrap Q HP columns (GE Healthcare) using 20 mmol • L⁻¹ Tris-HCl, pH 8.3; 1 mol • L⁻¹ NaCl and 6 mol • L⁻¹ urea as the elution buffer on linear 0-20% NaCl gradient⁸². Human APOA1 and APOA2 preparations were dialyzed against PBS and their purity was checked by SDS-polyacrylamide gel and Coomassie Blue staining and western-blot analyses using polyclonal antibodies directed against human APOA1 and APOA2 (Merck #178422 and Calbiochem #178464, respectively, not shown). The absence of cholesterol, phospholipids, triglycerides and sphingosine-1-phosphate in APOA1 and APOA2 preparations was verified (Table 1). APOA1, APOA2 and HDL₃ (used as a positive control) were prepared at 1 mg of protein per mL in PBS, then total cholesterol and triglycerides content was determined by the CHOD-PAP and GPO-PAP enzymatic colorimetric methods, respectively, using kits from Biolabo SA (Maizy, France). Phospholipids content was measured by choline-transformation method with spectrophotometric detection of choline-derived quinone end product (DiaSys Diagnostic Systems, Holzheim, Deutschland). Sphingosine-1-phosphate (S1P) was measured using liquid chromatography tandem mass spectrometry (LCMS). Briefly, 100 µL of samples were extracted according to modified acidic (HCl 2M) Bligh and Dyer method in the presence of Internal standard S1P (d20:1) (5 ng). Extracts were diazomethane-methylated in hexane at room temperature for 10 min before quenching reaction with acetic acid addition. After 6 min of centrifugation at 16,600 g, the supernatant was filtered, evaporated, and the final extract was solubilized in 20 µL of methanol. Quantification was done by ultra-performance liquid chromatography using a 1290 UPLC system coupled to a G6460 triple quadrupole spectrometer (Agilent) and an analytical column Acquity UPLC BEH C8 (Waters). Mobile phases A and B were composed respectively of H₂O 0.1% formic acid and acetonitrile 0.1% formic acid, in pressure solvent mode at 0.3 mL • min⁻¹ at 35 °C, with an injection volume of 5 µL.

Quantification was done in Selected Reaction Monitoring detection mode (SRM) with the transition 409-> 264 m/z for S1P and 437-> 293m/z for the internal standard, using a collision energy of 15eV, with calibration curves. Following infusion in mice, plasma human APOA1 level was assayed on an automated analyzer with an immunoturbidimetric method that does not cross-react with endogenous mouse APOA1 (Roche Diagnostics, France) and HDL-C was measured by enzymatic colorimetric method (HDL-cholesterol, Biolabo SA, Maizy, France).

4.6 – Inhibitory Factor 1 (IF1) production. The mature IF1 protein used in these experiments was 81 amino acid residues in length with histidine 49 switched to lysine, which is active at all pH values⁸³. This protein was chemically synthesized by GenScript (Piscataway, NJ, USA) at >90% purity.

4.7 - Placenta and umbilical cords. Human placentas and their umbilical cords were collected from 30 women immediately after placental delivery. All pregnancies were full term, and deliveries took place at the Service of Obstetrics and Gynecology, Guillermo Grant Benavente Hospital, Concepción, Chile. Women included in the study were 18–35 years old, had normal and single pregnancies, had normal fetal development, delivered at gestational age > 37 weeks and had a vaginal delivery or cesarean. The exclusion criteria for the participants included the presence of a previously established chronic disease in the woman, the presence of any pharmacological therapy, the presence of a medical or obstetrical complication during pregnancy and the presence of a metabolic or physical abnormality in the newborn. The placentas and umbilical cords were transported in sterile containers in PBS and were used within 6 h of their delivery.

4.8 - Western blot analysis. Confluent cells grown in 6-well culture plates were lysed in RIPA buffer and boiled for 5 min. Protein content was quantified by Pierce BCA Protein Assay Kit and total proteins were then separated on a 10% SDS-polyacrylamide gel (50 µg • well⁻¹) and transferred to a PVDF membrane (Immobilon-P, Millipore). After being blocked with 5% BSA in PBS buffer, the membranes were incubated overnight with specific antibodies. Anti-phospho-eNOS Ser¹¹⁷⁷ (R&D system #MAB9028; 5 µg • mL⁻¹), anti-eNOS total (BD Biosciences #610297; 0.25 µg • mL⁻¹), anti-P2Y₁ (Abcam #AB168918; 1 µg • mL⁻¹) and anti-P2Y₁₂ (Alomone #APR-020; 4 µg • mL⁻¹) were used. Membranes were then incubated with secondary horseradish peroxidase-conjugated anti-rabbit or anti-mouse (Promega #401B & #402B, respectively; 1 µg • mL⁻¹) for 1 h at room temperature, and immunoreactive proteins were visualized by ECL detection (Thermo Fisher Scientific) using the Chemidoc Imaging

system (Bio-Rad). Bands were quantified using Image Lab software (Bio-Rad). Values of phosphorylated eNOS were normalized against the amount of total eNOS. Changes in phosphorylation levels were evaluated by comparing the differences between basal (untreated cells) and stimulated (treated cells) values and were expressed as the fold increase over basal.

4.9 - eNOS activity. eNOS activity was measured as the amount of L-[³H]-arginine converted into L-[³H]-citrulline⁸⁴. HUVECs were seeded at a density of 25,000 cells • well⁻¹ in 24-well plates and were cultured in growth medium as described above until 80–90% confluent. Before experiments, the cells were serum-starved for 4 h, and then a mixture of APOA1 (concentration range: 25–200 µg • mL⁻¹, equivalent to 0.9–7.2 µmol • L⁻¹), L-[³H]-arginine (4 µCi • mL⁻¹, 5 mol • L⁻¹) and L-arginine (100 µmol • L⁻¹) was added to the cultures in M-199 medium without serum. In selected experiments, cells were incubated for 30 min with inhibitors of eNOS (L-NAME, 100 nmol • L⁻¹), ecto-F₁-ATPase (IF1, 1.8 µmol • L⁻¹; oligomycin, 125 nmol • L⁻¹), anti-ABCA1 (1:500), anti-SRBI (1:500), P2Y₁ (MRS2179, 10 µmol • L⁻¹) or P2Y₁₂ (cangrelor, 10 µmol • L⁻¹) before incubation with 50 µg • mL⁻¹ APOA1. In another set of experiments, dose-response assays were performed for ADP (10⁻² to 10³ µmol • L⁻¹) using the mixture of L-[³H]-arginine and L-arginine as described above. At the end of the incubation period with APOA1 or ADP (30 min), cells were washed with PBS and lysed with 0.5 mol • L⁻¹ KOH. As a positive control, cells were incubated with 1 mmol • L⁻¹ histamine instead of APOA1 or ADP. Lysates were resolved in a cation ion-exchange resin (Dowex 50WX8, Sigma-Aldrich), L-[³H]-citrulline radioactivity was normalized based on the protein content per well. Results were expressed as the fold change as compared with the basal condition (untreated cells).

4.10 - NO production. NO was detected using a DAF-FM-DA probe, which forms a fluorescent benzotriazole when it reacts with NO. HUVECs were seeded (10,000 cells • well⁻¹) in 96-well plates and cultured in growth medium as described above until 80–90% confluent. The medium was then replaced with M-199 without serum for 4 h, and the cells were incubated for 30 min with DAF-FM-DA (5 µmol • L⁻¹) diluted in PBS. APOA1 (50 µg • mL⁻¹) was added, and the fluorescence was recorded for 30 min ($\lambda_{ex} = 495 \text{ nm}$, $\lambda_{em} = 515 \text{ nm}$) with a Tecan Flash Multimode Reader (Thermo Fisher Scientific). As a positive control, 1 mmol • L⁻¹ histamine was added instead of APOA1 (not shown). In another set of experiments, cells were incubated with inhibitors for 30 min before treatment with APOA1. Fluorescence for each condition was compared with the value obtained in untreated cells, and results were expressed

as the fold change as compared with the basal condition (untreated cells).

4.11 - Real-time NO production. After lethal anesthesia of 8- to 9-week-old mice (n = 5 per group) with intraperitoneal injection of ketamine hydrochloride (365 µmol • kg⁻¹) and xylazine hydrochloride (58 µmol • kg⁻¹), aortas were quickly harvested and maintained in 400 µL Krebs-Ringer oxygenated solution (mmol • L⁻¹: NaCl 119, KCl 4.6, MgCl₂ 1.2, KH₂PO₄ 1.2, CaCl₂ 1.5, NaHCO₃ 15 and glucose 2.5; pH 7.4) at 37°C. A NO-specific amperometric probe (ISO-NOPF100; World Precision Instrument or WPI, Sarasota, FL) was implanted directly in the tissue, and NO release was monitored in real time. The NO concentration was measured with the data acquisition system Lab Trax (WPI) connected to the free radical analyzer Apollo 1000 (WPI). The NO-specific amperometric probe was calibrated as described⁸⁵. Aortas were exposed to PBS, 25 or 50 µg • mL⁻¹ APOA1, and NO production was continuously monitored for 10 min. In a separate set of experiments, we co-exposed the aortas to APOA1 (50 µg • mL⁻¹, equivalent to 1.8 µmol • L⁻¹) together with L-NMMA (500 µmol • L⁻¹), IF1 (3.6 µmol • L⁻¹), MRS2179 (50 µmol • L⁻¹) or Cangrelor (50 µmol • L⁻¹). Data acquisition and analysis were performed with DataTrax2 software (WPI). Results were expressed as the difference in NO release relative to the basal condition (before stimulation with pharmacological agents).

4.12 - Immunohistochemistry. Mouse aortas were harvested and maintained at 37°C in Krebs-Ringer as described above. Aortas were incubated with APOA1 (50 µg • mL⁻¹) for 10 min with or without prior treatment with IF1 (1.8 µmol • L⁻¹) for 10 min. The control group was treated with PBS or IF1 (1.8 µmol • L⁻¹) for the whole experiment. At the end of the stimulation, aortas were fixed immediately in buffered 4% formalin and embedded in paraffin, and sections perpendicular to the long axis of the vessel were cut. One serial section from each set was subjected to standard hematoxylin/eosin staining. On the other sections, immunostaining was performed with a polyclonal phospho-Ser¹¹⁷⁷-eNOS antibody (1:500; Sigma-Aldrich) overnight at 4°C after wet autoclaving of the sections with 0.01 mol • L⁻¹ citrate buffer (pH 6.0) for 10 min at 95°C. Detection was performed at room temperature using biotinylated goat anti-rabbit (1:250) for 30 min followed by the development of the chromogen reaction using the HRP/DAB detection kit (Vector Laboratories). Sections were counterstained with hematoxylin. Images of the immunostained sections were taken with a Panoramic 250 FLASH II Scanner (3DHISTECH, Budapest, Hungary) using scanner software 1.17 and Panoramic Viewer 1.15.4.

4.13 - Human vein reactivity. Human umbilical veins and chorionic veins (referred to as placental veins) were isolated

and carefully dissected from surrounding connective tissue. The dissected vein was cut transversely to produce rings 2–4 mm in length. The dissection was done with extreme care to protect the endothelium from inadvertent damage. For some experiments, the endothelial layer was mechanically removed from the rings by gently rubbing the luminal surface of the vessel with a roughened glass rod⁸⁴. Each ring was then mounted on a wire myograph (610M Multiwire Myograph System, Danish Myo Technology A/S, Denmark) in an organ bath containing Krebs-Ringer solution at 37°C and continuously aerated with 95% O₂ and 5% CO₂. Vessel tension was adjusted manually to 1 g, then, following 1 h of stabilization, reactivity was confirmed by inducing constriction with a Krebs-potassium solution containing 124 mmol • L⁻¹ KCl. Once the maximal response to KCl was obtained, rings were washed with Krebs-Ringer solution and stabilized again for 1h. For experiments, vasoconstriction was induced with 100 nmol • L⁻¹ U46619, a chemical and stable agonist of thromboxane A₂ receptors that produces vasoconstriction in an endothelium-independent fashion, by activating thromboxane/prostaglandin (TP) receptors on smooth muscle cells^{77,86}. After 15 min of incubation with U46619, 50 µg • mL⁻¹ APOA1 or PBS (control) was added to the bath, and changes in isometric tension were recorded for 20 min using a PowerLab 8/30 Data Acquisition System coupled to LabChart 6 software (AD Instruments, Australia). In selected studies, intact human vein rings were pre-incubated with L-NAME (200 µmol • L⁻¹) or IF1 (1.8 µmol • L⁻¹) for 45 min, and their subsequent response to 50 µg • mL⁻¹ APOA1 (equivalent to 1.8 µmol • L⁻¹) was measured. Considering T₀ (t = 0 min) as the time when APOA1 or PBS was added to the bath, the vasoconstriction response for each treatment at each time point was expressed as the percentage of the maximal contraction caused by 124 mmol • L⁻¹ KCl⁸⁷, and was further normalized to the percentage of constriction at T₀.

4.14 - Blood flow and heart rate measurements on mice.

Blood flow measurements were performed on 13- to 18-week-old mice. All surgical procedures were done under anesthesia with isoflurane (1.5%) with a flow rate of 0.2 L • min⁻¹. No analgesia was required for these surgical procedures. Briefly, 10 d before experimentation, an intravenous catheter was introduced into the left femoral vein, sealed under the skin and externalized at the back of the neck. Mice were allowed to recover for 6 d before an ultrasonic probe measuring blood flow and heart rate (Transonic System, Emka Technologies, Inc., Paris, France) was inserted around the right femoral artery. The probe wire was sealed under the skin at the back of the neck, where it was secured using surgical thread⁸⁸. After surgery, mice were returned to their cages for 4-5 d until their body weight

recovered. Animals that did not reach their pre-surgery weight (<15% of the total number) were excluded from the study. On the experimental day, mice were starved for 3 h. The average mean weight after the fasting period was 27.6 ± 0.2 g. The probe was connected to a Transonic model T403 Flowmeter (Transonic System), and basal blood flow (mL • min⁻¹) and heart rate (beats per min, b.p.m.) were recorded for 1 h in awake and freely moving mice. Then, treatments were performed by continuous infusions for 30 min at 6 µL • min⁻¹ of PBS (control), L-NMMA (0.7 µmol • kg⁻¹ • min⁻¹), IF1 (60 nmol • kg⁻¹ • min⁻¹) or MRS2179 (0.7 µmol • kg⁻¹ • min⁻¹), followed by an additional 45 min with or without human APOA1 (30 nmol • kg⁻¹ • min⁻¹). In another set of experiments, treatments were performed by continuous infusions for 20 min at 2 µL • min⁻¹ of PBS (control), L-NMMA (1.5 µmol • kg⁻¹ • min⁻¹) or MRS2179 (1.5 µmol • kg⁻¹ • min⁻¹), followed by an additional 20 min with or without 2meSADP (0.7 µmol • kg⁻¹ • min⁻¹). For each experimental group, the baseline blood flow (mL • min⁻¹) was the mean of blood flow values measured for 2 min, before the T₀ time point when starts infusion of APOA1 or 2meSADP. Within experimental groups, no statistical difference in baseline blood flow was observed between the different treatment conditions (Table 2). Results are expressed as the percentage change from the mean basal blood flow and heart rate and are reported on separate graphs for each treatment condition.

4.15 - Data analysis and statistics. Data are expressed as the mean ± SEM. Data were analyzed using GraphPad Prism version 5.00 for Windows (GraphPad Software, San Diego, CA) for statistical significance by applying a one- or two-way analysis of variance followed by a *post hoc* Bonferroni multiple comparison test. The level of significance was defined as p < 0.05.

ACKNOWLEDGMENTS

We thank the Service of Obstetrics and Gynecology, Guillermo Grant Benavente Hospital, Concepción, for the kind support in obtaining human placenta and umbilical cords. We also thank Dr. Katia Sáez, Mathematical Engineer and Master in Statistics, Faculty of Physical and Mathematical Sciences, Universidad de Concepción, for statistical analysis support. Immunohistochemistry experiments were performed at the Experimental Histopathology facility of INSERM/UPS US006 CREFRE (Toulouse, France), and we thank Florence Capilla, Annie Alloy and Talal Al Saati for their technical assistance. APOA1 and APOA2 preparations were performed at the Functional Biochemistry Facility “We-Met” (Alexandre Lucas, I2MC, Toulouse, France). S1P quantification was done at the MetaToul-Lipidomique Core Facility (I2MC, Inserm 1048, Toulouse, France), MetaboHUB-ANR-11-INBS-0010. We thanks Arielle Noirot for technical assistance in experimental studies with animals, Animal core facility, Faculty of Pharmacy, University Paul Sabatier, Toulouse.

FUNDING INFORMATION

This work was supported by the “Fondo Nacional de Desarrollo Científico y Tecnológico” (FONDECYT, #11121575, Chile), “Dirección de Investigación Universidad de Concepción” (DIUC, #210.072.033-1.0, Chile), the French National Research Agency (ANR, #ANR-16-CE18-0014-01, HDL-NEXT-THERAPEUTICS) and the “Région Midi-Pyrénées - Occitanie” (CLE 2015, #14054132). “INNOVA BIO BIO Chile para Apoyo de Tesis” fellowships were held by P. Honorato (#13.1285-EM.TES) and M. León (#12.127-EM.TES). L. Briceño was supported by “Comisión Nacional de Investigación Científica y Tecnológica CONICYT-PCHA/Magíster Nacional” (#2014-63566), Chile.

CONFLICT OF INTEREST

None

REFERENCES

1. Vanhoutte PM, Shimokawa H, Feletou M, Tang EHC. Endothelial dysfunction and vascular disease – a 30th anniversary update. *Acta Physiol.* 2017;219(1):22-96.
2. Farah C, Michel LYM, Balligand J-L. Nitric oxide signalling in cardiovascular health and disease. *Nat Rev Cardiol.* 2018;15(5):292-316.
3. Ramet ME, Ramet M, Lu Q, et al. High-density lipoprotein increases the abundance of eNOS protein in human vascular endothelial cells by increasing its half-life. *J Am Coll Cardiol.* 2003;41(12):2288-2297.
4. Kuvin JT, Ramet ME, Patel AR, Pandian NG, Mendelsohn ME, Karas RH. A novel mechanism for the beneficial vascular effects of high-density lipoprotein cholesterol: enhanced vasorelaxation and increased endothelial nitric oxide synthase expression. *Am Hear J.* 2002;144(1):165-172.
5. Mineo C, Yuhanna IS, Quon MJ, Shaul PW. High density lipoprotein-induced endothelial nitric-oxide synthase activation is mediated by Akt and MAP kinases. *J Biol Chem.* 2003;278(11):9142-9149.
6. Nofer JR, van der Giet M, Tolle M, et al. HDL induces NO-dependent vasorelaxation via the lysophospholipid receptor S1P3. *J Clin Invest.* 2004;113(4):569-581.
7. Besler C, Heinrich K, Rohrer L, et al. Mechanisms underlying adverse effects of HDL on eNOS-activating pathways in patients with coronary artery disease. *J Clin Invest.* 2011;121(7):2693-2708.
8. Carvalho LSF, Panzoldo N, Santos SN, et al. HDL levels and oxidizability during myocardial infarction are associated with reduced endothelial-mediated vasodilation and nitric oxide bioavailability. *Atherosclerosis.* 2014;237(2):840-846.
9. Spieker LE, Sudano I, Hürlimann D, et al. High-density lipoprotein restores endothelial function in hypercholesterolemic men. *Circulation.* 2002;105(12):1399-1402.
10. Basisoendial RJ, Hovingh GK, Levels JH, et al. Restoration of endothelial function by increasing high-density lipoprotein in subjects with isolated low high-density lipoprotein. *Circulation.* 2003;107(23):2944-2948.
11. Yuhanna IS, Zhu Y, Cox BE, et al. High-density lipoprotein binding to scavenger receptor-BI activates endothelial nitric oxide synthase. *Nat Med.* 2001;7(7):853-857.
12. Li X. A. 2002Li, Titlow WB, Jackson BA, et al. High density lipoprotein binding to scavenger receptor, Class B, type I activates endothelial nitric-oxide synthase in a ceramide-dependent manner. *J Biol Chem.* 2002;277(13):11058-11063.
13. Gong M, Wilson M, Kelly T, et al. HDL-associated estradiol stimulates endothelial NO synthase and vasodilation in an SR-BI-dependent manner. *J Clin Invest.* 2003;111(10):1579-1587.
14. Asztalos BF, Roheim PS. Presence and formation of “free apolipoprotein A-I-like” particles in human plasma. *Arter Thromb Vasc Biol.* 1995;15(9):1419-1423.
15. Barrans A, Collet X, Barbaras R, et al. Hepatic lipase induces the formation of pre-β1 high density lipoprotein (HDL) from triacylglycerol-rich HDL2. *J Biol Chem.* 1994;269:11572-11577.
16. Jaspard B, Collet X, Barbaras R, et al. Biochemical characterization of pre-b1 high-density lipoprotein from human ovarian follicular fluid: evidence for the presence of a lipid core. *Biochemistry.* 1996;35:1352-1357.
17. Rye KA, Barter PJ. Formation and metabolism of prebeta-migrating, lipid-poor apolipoprotein A-I. *Arter Thromb Vasc Biol.* 2004;24(3):421-428.
18. Drew BG, Fidge NH, Gallon-Beaumier G, Kemp BE, Kingwell BA. High-density lipoprotein and apolipoprotein AI increase endothelial NO synthase activity by protein association and multisite phosphorylation. *Proc Natl Acad Sci U S A.* 2004;101(18):6999-7004.
19. Ou J, Wang J, Xu H, et al. Effects of D-4F on vasodilation and vessel wall thickness in hypercholesterolemic LDL receptor-null and LDL receptor/apolipoprotein A-I double-knockout mice on Western diet. *Circ Res.* 2005;97(11):1190-1197.
20. Martinez LO, Jacquet S, Esteve JP, et al. Ectopic beta-chain of ATP synthase is an apolipoprotein A-I receptor in hepatic HDL endocytosis. *Nature.* 2003;421(6918):75-79.
21. Radojkovic C, Genoux A, Pons V, et al. Stimulation of Cell Surface F1-ATPase Activity by Apolipoprotein A-I Inhibits Endothelial Cell Apoptosis and Promotes Proliferation. *Arter Thromb Vasc Biol.* 2009;29(7):1125-1130.
22. Cavellier C, Ohnsorg PM, Rohrer L, von Eckardstein A. The beta-Chain of Cell Surface F0F1 ATPase Modulates ApoA-I and HDL Transcytosis Through Aortic Endothelial Cells. *Arter Thromb Vasc Biol.* 2012;32(1):131-139.
23. González-Pecchi V, Valdés S, Pons V, et al. Apolipoprotein A-I enhances proliferation of human endothelial progenitor cells and promotes angiogenesis through the cell surface ATP synthase. *Microvasc Res.* 2015;98:9-15.
24. Martinez LO, Najib S, Perret B, Cabou C, Lichtenstein L. Ecto-F1-ATPase/P2Y pathways in metabolic and vascular functions of high density lipoproteins. *Atherosclerosis.* 2015;238(1):89-100.
25. Fabre ACA, Malaval C, Ben Addi A, et al. P2Y13 receptor is critical for reverse cholesterol transport. *Hepatology.* 2010;52(4):1477-1483.
26. Serhan N, Cabou C, Verdier C, et al. Chronic pharmacological activation of P2Y13 receptor in mice decreases

- HDL-cholesterol level by increasing hepatic HDL uptake and bile acid secretion. *Biochim Biophys Acta - Mol Cell Biol Lipids*. 2013;1831(4):719-725.
27. Castaing-Berthou A, Malet N, Radojkovic C, et al. PI3K β Plays a Key Role in Apolipoprotein A-I-Induced Endothelial Cell Proliferation Through Activation of the Ecto-F₁-ATPase/P2Y₁ Receptors. *Cell Physiol Biochem*. 2017;42(2):579-593.
 28. da Silva CG, Jarzyna R, Specht A, Kaczmarek E. Extracellular nucleotides and adenosine independently activate AMP-activated protein kinase in endothelial cells: involvement of P₂ receptors and adenosine transporters. *Circ Res*. 2006;98(5):e39-47.
 29. Wang S, Iring A, Strilic B, et al. P₂Y₂ and Gq/G11 control blood pressure by mediating endothelial mechanotransduction. *J Clin Invest*. 2015;125(8):3077-3086.
 30. Wihlborg A-K, Malmström M, Eijolfsson A, Gustafsson R, Jacobson K, Erlinge D. Extracellular nucleotides induce vasodilatation in human arteries via prostaglandins, nitric oxide and endothelium-derived hyperpolarising factor. *Br J Pharmacol*. 2003;138(8):1451-1458.
 31. Guns PJ, Van Assche T, Franssen P, Robaye B, Boeynaems JM, Bult H. Endothelium-dependent relaxation evoked by ATP and UTP in the aorta of P₂Y₂-deficient mice. *Br J Pharmacol*. 2006;147(5):569-574.
 32. Guns P-JDF, Korda A, Crauwels HM, et al. Pharmacological characterization of nucleotide P₂Y receptors on endothelial cells of the mouse aorta. *Br J Pharmacol*. 2005;146(2):288-295.
 33. Yamamoto K, Sokabe T, Matsumoto T, et al. Impaired flow-dependent control of vascular tone and remodeling in P₂X₄-deficient mice. *Nat Med*. 2006;12(1):133-137.
 34. Mount PF, Kemp BE, Power DA. Regulation of endothelial and myocardial NO synthesis by multi-site eNOS phosphorylation. *J Mol Cell Cardiol*. 2007;42(2):271-279.
 35. Bason J V., Runswick MJ, Fearnley IM, Walker JE. Binding of the inhibitor protein IF1 to bovine F₁-ATPase. *J Mol Biol*. 2011;406(3):443-453.
 36. Mangiullo R, Gnoni A, Leone A, Gnoni G V, Papa S, Zanotti F. Structural and functional characterization of F₁F₀-ATP synthase on the extracellular surface of rat hepatocytes. *Biochim Biophys Acta*. 2008;1777(10):1326-1335.
 37. Lee T-S, Pan C-C, Peng C-C, et al. Anti-atherogenic effect of berberine on LXR α -ABCA1-dependent cholesterol efflux in macrophages. *J Cell Biochem*. 2010;111(1):104-110.
 38. Sharma M, Von Zychlinski-Kleffmann A, Porteous CM, Jones GT, Williams MJA, McCormick SPA. Lipoprotein (a) upregulates ABCA1 in liver cells via scavenger receptor-B1 through its oxidized phospholipids. *J Lipid Res*. 2015;56(7):1318-1328.
 39. Wang L, Karlsson L, Moses S, et al. P₂ receptor expression profiles in human vascular smooth muscle and endothelial cells. *J Cardiovasc Pharmacol*. 2002;40(6):841-853.
 40. Shen J, DiCorleto PE. ADP stimulates human endothelial cell migration via P₂Y₁ nucleotide receptor-mediated mitogen-activated protein kinase pathways. *Circ Res*. 2008;102(4):448-456.
 41. Hechler B, Gachet C. P₂ receptors and platelet function. *Purinergic Signal*. 2011;7(3):293-303.
 42. Suplat D, Krzemiński P, Pomorski P, Barańska J. P₂Y₁ and P₂Y₁₂ receptor cross-talk in calcium signalling: Evidence from nonstarved and long-term serum-deprived glioma C6 cells. *Purinergic Signal*. 2007;3(3):221-230.
 43. Yoshioka K, Saitoh O, Nakata H. Agonist-promoted heteromeric oligomerization between adenosine A₁ and P₂Y₁ receptors in living cells. *FEBS Lett*. 2002;523(1-3):147-151.
 44. Da Silva CG, Specht A, Wegiel B, Ferran C, Kaczmarek E. Mechanism of purinergic activation of endothelial nitric oxide synthase in endothelial cells. *Circulation*. 2009;119(6):871-879.
 45. Hess CN, Kou R, Johnson RP, Li GK, Michel T. ADP signaling in vascular endothelial cells: ADP-dependent activation of the endothelial isoform of nitric-oxide synthase requires the expression but not the kinase activity of AMP-activated protein kinase. *J Biol Chem*. 2009;284(47):32209-32224.
 46. Bender SB, Berwick ZC, Laughlin MH, Tune JD. Functional contribution of P₂Y₁ receptors to the control of coronary blood flow. *J Appl Physiol*. 2011;111(6):1744-1750.
 47. Wareing M, Greenwood SL, Taggart MJ, Baker PN. Vasoactive responses of veins isolated from the human placental chorionic plate. *Placenta*. 2003;24(7):790-796.
 48. Furchgott RF, Zawadzki J V. The obligatory role of endothelial cells in the relaxation of arterial smooth muscle by acetylcholine. *Nature*. 1980;288(5789):373-376.
 49. Spiers A, Padmanabhan N. A guide to wire myography. *Methods Mol Med*. 2005;108:91-104.
 50. Jacquet S, Malaval C, Martinez LO, et al. The nucleotide receptor P₂Y₁₃ is a key regulator of hepatic high-density lipoprotein (HDL) endocytosis. *Cell Mol Life Sci*. 2005;62(21):2508-2515.
 51. Malaval C, Laffargue M, Barbaras R, et al. RhoA/ROCK I signalling downstream of the P₂Y₁₃ ADP-receptor controls HDL endocytosis in human hepatocytes. *Cell Signal*. 2009;21(1):120-127.
 52. Lichtenstein L, Serhan N, Annema W, et al. Lack of P₂Y₁₃ in mice fed a high cholesterol diet results in decreased hepatic cholesterol content, biliary lipid secretion and reverse cholesterol transport. *Nutr Metab*. 2013;10(1):67-73.

53. Lichtenstein L, Serhan N, Espinosa-Delgado S, et al. Increased Atherosclerosis in P2Y13 / Apolipoprotein E Double-Knockout Mice: Contribution of P2Y13 to Reverse Cholesterol Transport. *Cardiovasc Res.* 2015;106(2):315-323.
54. Lohman AW, Billaud M, Isakson BE. Mechanisms of ATP release and signalling in the blood vessel wall. *Cardiovasc Res.* 2012;95(3):269-280.
55. Hellsten Y, Maclean D, Rådegran G, Saltin B, Bangsbo J. Adenosine concentrations in the interstitium of resting and contracting human skeletal muscle. *Circulation.* 1998;98(1):6-8.
56. Fu Y, Hou Y, Fu C, et al. A novel mechanism of γ/δ T-lymphocyte and endothelial activation by shear stress: the role of ecto-ATP synthase β chain. *Circ Res.* 2011;108(4):410-417.
57. Bharath LP, Cho JM, Park S-K, et al. Endothelial Cell Autophagy Maintains Shear Stress-Induced Nitric Oxide Generation via Glycolysis-Dependent Purinergic Signaling to Endothelial Nitric Oxide Synthase. *Arterioscler Thromb Vasc Biol.* 2017;37(9):1646-1656.
58. Wijeyeratne YD, Heptinstall S. Anti-platelet therapy: ADP receptor antagonists. *Br J Clin Pharmacol.* 2011;72(4):647-657.
59. Heiss EH, Dirsch VM. Regulation of eNOS enzyme activity by posttranslational modification. *Curr Pharm Des.* 2014;20(22):3503-3513.
60. Igarashi J, Michel T. Sphingosine 1-phosphate and isoform-specific activation of phosphoinositide 3-kinase beta. Evidence for divergence and convergence of receptor-regulated endothelial nitric-oxide synthase signaling pathways. *J Biol Chem.* 2001;276(39):36281-36288.
61. Uruno A, Sugawara A, Kanatsuka H, et al. Upregulation of nitric oxide production in vascular endothelial cells by all-trans retinoic acid through the phosphoinositide 3-kinase/Akt pathway. *Circulation.* 2005;112(5):727-736.
62. Tran-Dinh A, Diallo D, Delbosc S, et al. HDL and endothelial protection. *Br J Pharmacol.* 2013;169(3):493-511.
63. Terasaka N, Yu S, Yvan-Charvet L, et al. ABCG1 and HDL protect against endothelial dysfunction in mice fed a high-cholesterol diet. *J Clin Invest.* 2008;118(11):3701-3713.
64. Mulya A, Lee J-Y, Gebre AK, Thomas MJ, Colvin PL, Parks JS. Minimal lipidation of pre-beta HDL by ABCA1 results in reduced ability to interact with ABCA1. *Arterioscler Thromb Vasc Biol.* 2007;27(8):1828-1836.
65. Vedhachalam C, Ghering AB, Davidson WS, Lund-Katz S, Rothblat GH, Phillips MC. ABCA1-induced cell surface binding sites for ApoA-I. *Arterioscler Thromb Vasc Biol.* 2007;27(7):1603-1609.
66. Vaisman BL, Demosky SJ, Stonik JA, et al. Endothelial expression of human ABCA1 in mice increases plasma HDL cholesterol and reduces diet-induced atherosclerosis. *J Lipid Res.* 2012;53(1):158-167.
67. Cavellier C, Rohrer L, von Eckardstein A. ATP-Binding cassette transporter A1 modulates apolipoprotein A-I transcytosis through aortic endothelial cells. *Circ Res.* 2006;99(10):1060-1066.
68. Miyazaki O, Ogiwara J, Fukamachi I, Kasumi T. Evidence for the presence of lipid-free monomolecular apolipoprotein A-1 in plasma. *J Lipid Res.* 2014;55(2):214-225.
69. Nanjee MN, Brinton EA. Very small apolipoprotein A-I-containing particles from human plasma: isolation and quantification by high-performance size-exclusion chromatography. *Clin Chem.* 2000;46(2):207-223.
70. Jaspard B, Fournier N, Vieitez G, et al. Structural and functional comparison of HDL from homologous human plasma and follicular fluid. A model for extravascular fluid. *Arter Thromb Vasc Biol.* 1997;17(8):1605-1613.
71. Shao B. Site-specific oxidation of apolipoprotein A-I impairs cholesterol export by ABCA1, a key cardioprotective function of HDL. *Biochim Biophys Acta.* 2012;1821(3):490-501.
72. Huang Y, DiDonato JA, Levison BS, et al. An abundant dysfunctional apolipoprotein A1 in human atheroma. *Nat Med.* 2014;20(2):193-203.
73. DiDonato JA, Aulak K, Huang Y, et al. Site-specific nitration of apolipoprotein A-I at tyrosine 166 is both abundant within human atherosclerotic plaque and dysfunctional. *J Biol Chem.* 2014;289(15):10276-10292.
74. Lang I, Pabst MA, Hiden U, et al. Heterogeneity of microvascular endothelial cells isolated from human term placenta and macrovascular umbilical vein endothelial cells. *Eur J Cell Biol.* 2003;82(4):163-173.
75. Sobrevia L, Abarzúa F, Nien JKK, et al. Review: Differential placental macrovascular and microvascular endothelial dysfunction in gestational diabetes. *Placenta.* 2011;32(SUPPL. 2):S159-S164.
76. Errasti AE, Luciani LI, Cesio CE, et al. Potentiation of adrenaline vasoconstrictor response by sub-threshold concentrations of U-46619 in human umbilical vein: involvement of smooth muscle prostanoid TP(alpha) receptor isoform. *Eur J Pharmacol.* 2007;562(3):227-235.
77. Ellinsworth DC, Shukla N, Fleming I, Jeremy JY. Interactions between thromboxane A₂, thromboxane/prostaglandin (TP) receptors, and endothelium-derived hyperpolarization. *Cardiovasc Res.* 2014;102(1):9-16.
78. Fielding PE, Nagao K, Hakamata H, Chimini G, Fielding CJ. A two-step mechanism for free cholesterol and phospholipid efflux from human vascular cells to apolipoprotein A-1. *Biochemistry.* 2000;39(46):14113-20.
79. Ishida K, Matsumoto T, Taguchi K, Kamata K, Kobayashi T. Mechanisms underlying reduced P2Y(1)-receptor-mediated relaxation in superior mesenteric arteries from long-term streptozotocin-induced diabetic rats. *Acta Physiol (Oxf).* 2013;207(1):130-141.

80. Havel RJ, Eder HA, Bragdon JR. The distribution and chemical composition of ultracentrifugally separated lipoproteins in human serum. *J Clin Invest*. 1955;34:1345-1353.
81. Bligh EG, Dyer WJ. A rapid method of total lipid extraction and purification. *Can J Biochem Physiol*. 1959;37(8):911-917.
82. Martinez LO, Georgeaud V, Rolland C, et al. Characterization of Two High-Density Lipoprotein Binding Sites on Porcine Hepatocyte Plasma Membranes: Contribution of Scavenger Receptor Class B Type I (SR-BI) to the Low-Affinity Component. *Biochemistry*. 2000;39(5):1076-1082.
83. Cabezon E, Butler PJ, Runswick MJ, Walker JE. Modulation of the oligomerization state of the bovine F1-ATPase inhibitor protein, IF1, by pH. *J Biol Chem*. 2000;275(33):25460-4.
84. González M, Gallardo V, Rodríguez N, et al. Insulin-stimulated L-arginine transport requires SLC7A1 gene expression and is associated with human umbilical vein relaxation. *J Cell Physiol*. 2011;226(11):2916-2924.
85. Duparc T, Colom A, Cani PD, et al. Central Apelin Controls Glucose Homeostasis via a Nitric Oxide-Dependent Pathway in Mice. *Antioxid Redox Signal*. 2011;15(6):1477-1496.
86. Abramovitz M, Adam M, Boie Y, et al. The utilization of recombinant prostanoid receptors to determine the affinities and selectivities of prostaglandins and related analogs. *Biochim Biophys Acta*. 2000;1483(2):285-293.
87. González M, Rojas S, Avila P, et al. Insulin reverses D-glucose-increased nitric oxide and reactive oxygen species generation in human umbilical vein endothelial cells. *PLoS One*. 2015;10(4):1-23.
88. Cabou C, Campistron G, Marsollier N, et al. Brain glucagon-like peptide-1 regulates arterial blood flow, heart rate, and insulin sensitivity. *Diabetes*. 2008;57(10):2577-2587.

Table 1. Quantification of phospholipids, cholesterol, triglycerides and sphingosine-1-phosphate in APOA1, APOA2 and HDL₃ preparations.

	Phospholipids (mg • dL ⁻¹)	Cholesterol (mg • dL ⁻¹)	Triglycerides (mg • dL ⁻¹)	Sphingosine-1-phosphate (pmol per mg protein)
APOA1	<i>n.d.</i>	<i>n.d.</i>	<i>n.d.</i>	<i>n.d.</i>
APOA2	<i>n.d.</i>	<i>n.d.</i>	<i>n.d.</i>	<i>n.d.</i>
HDL ₃	24.97	30.67	4.96	269.12*

APOA1, APOA2 and HDL₃ were prepared at 1mg of protein • mL⁻¹ for lipid quantification.

**S1P in HDL / protein in HDL

n.d. : not detected

Table 2. Baseline mean blood flow in experimental groups of mice.

Experimental groups with apoA1	PBS (n = 9)	APOA1 (n = 6)	L-NMMA (n=6)	L-NMMA + APOA1 (n = 6)	IF1 (n = 7)	IF1 + APOA1 (n = 9)	MRS2179 (n = 7)	MRS2179 + APOA1 (n = 7)
mL • min ⁻¹	0.29±0.03	0.29±0.04	0.27±0.04	0.29±0.06	0.25±0.03	0.33±0.03	0.27±0.03	0.26±0.02

Experimental groups with 2meSADP	PBS (n = 5)	2meSADP (n = 4)	L-NMMA (n=4)	L-NMMA + 2meSADP (n = 6)	MRS2179 (n = 4)	MRS2179 + 2meADP (n = 5)
mL • min ⁻¹	0.23±0.03	0.17±0.02	0.25±0.04	0.24±0.03	0.31 ± 0.07	0.32±0.04

For each experimental group, baseline blood flow values are the mean of blood flow values measured for 2 min, before the T0 time point when starts infusion of APOA1 or 2meSADP. Values are expressed as mean ± SEM. Within experimental groups, no statistical difference was observed between the different treatment conditions.

FIGURE LEGENDS

Figure 1: APOA1 increases eNOS activity and NO production in human endothelial cells and mouse aortas. Endothelial NOS activity was quantified in HUVECs by measuring the conversion of L-[³H]-arginine to L-[³H]-citrulline for 30 min. Nitric oxide production in HUVECs was measured by using the NO-sensitive fluorescence probe DAF-FM-DA. NO release from mouse aortas was evaluated *ex vivo* by amperometric measurement. **A)** eNOS activity in the presence of increasing concentrations of APOA1. **B)** eNOS activity under the basal condition or in the presence of APOA1 (50 µg • mL⁻¹) with or without prior treatment with L-NAME (100 nmol • L⁻¹). **C)** Time course of NO production under the basal condition (PBS) or in the presence of APOA1 (50 µg • mL⁻¹). **D)** NO production under the basal condition or in the presence of APOA1 (50 µg • L⁻¹) with or without prior treatment with L-NAME (100 nmol • L⁻¹). APOA2 (50 µg • L⁻¹) was used as a control. **E)** Real-time NO release in aortas incubated for 10 min with 25 or 50 µg • mL⁻¹ APOA1 or vehicle (PBS). **F)** Measurement of real-time NO release from aortas incubated with APOA1 (50 µg • mL⁻¹) or vehicle (PBS) with or without L-NMMA (500 µmol • L⁻¹). n = 3 independent experiments, each condition in triplicate (A, B, C, D); n = 5–7 independent experiments for each condition (E, F). * p<0.05, † p<0.01, and ‡ p<0.001 compared to the control without APOA1 (PBS alone) or as indicated. NS indicates not significant (p ≥ 0.05).

Figure 2: APOA1 increases eNOS phosphorylation at serine 1177 through the activation of ecto-F₁-ATPase. **A)** eNOS phosphorylation (p-Ser¹¹⁷⁷) was assessed in HUVECs incubated with APOA1 (50 µg • mL⁻¹) for different times. **B)** Measurement of eNOS phosphorylation in HUVECs pre-incubated for 30 min with IF1 (1.8 µmol • L⁻¹), then stimulated for 30 min with APOA1 (50 µg • mL⁻¹). **C,** Representative images of phospho-Ser¹¹⁷⁷-eNOS in the endothelial lining of mouse aortic sections (n = 6 aortas per each condition). Aortas were incubated with APOA1 (50 µg • mL⁻¹) for 10 min with or without prior treatment with IF1 (1.8 µmol • L⁻¹) for 10 min. The control group was treated with PBS or IF1 alone (1.8 µmol • L⁻¹). Arrows indicate phospho-eNOS staining in the endothelial lining (original magnification, ×200, scale bare indicates 100 µm). Immunoblots are representative of three independent experiments. * p<0.05 and † p<0.01 compared to the control without APOA1 (PBS alone) or as indicated.

Figure 3: APOA1–induced eNOS activation and endothelial NO production occurs through ecto-F₁-ATPase. **A)** eNOS activity under the basal condition or in the presence of APOA1 (50 µg • mL⁻¹) with or without prior treatment with IF1 (1.8 µmol • L⁻¹) or Oligomycin (125 nmol • L⁻¹). **B)** NO production under the conditions as in A. **C)** Measurement of real-time NO release from aortas incubated with APOA1 (50 µg • mL⁻¹) or vehicle (PBS) with or without IF1 (3.6 µmol • L⁻¹). **D)** eNOS activity under the basal condition or in the presence of APOA1 (50 µg • mL⁻¹) with or without prior treatment (30 min) with neutralizing antibody directed against ABCA1 (1:500). **E)** eNOS activity under the basal condition or in the presence of APOA1 (50 µg • mL⁻¹) or HDL (50 µg • mL⁻¹) with or without prior treatment (30 min) with neutralizing antibody directed against SR-BI (1:500). n = 3 independent experiments, each condition in triplicate (A, B, D, E); n = 5–7 independent experiments for each condition (C). † p<0.01 and ‡ p<0.001 compared to the control without APOA1 (PBS alone) or as indicated. NS indicates not significant (p ≥ 0.05).

Figure 4: P2Y₁ receptor mediates eNOS activity and endothelial NO production in response to APOA1 stimulation. **A)** Expression of P2Y₁ and P2Y₁₂ in HUVECs and human platelets. Cellular extracts from HUVECs were from two donors. MW: molecular weight marker. **B)** Measurement of eNOS activity in HUVECs incubated for 30 min with increasing concentrations of ADP. **C-D)** eNOS activity and NO production in HUVECs under the basal condition or in the presence

of APOA1 ($50 \mu\text{g} \cdot \text{mL}^{-1}$) with or without prior treatment with MRS2179 ($10 \mu\text{mol} \cdot \text{L}^{-1}$) or cangrelor ($10 \mu\text{mol} \cdot \text{L}^{-1}$). **E** Measurement of real-time NO release from aortas incubated with APOA1 ($50 \mu\text{g} \cdot \text{mL}^{-1}$) or vehicle (PBS) with or without MRS2179 ($50 \mu\text{mol} \cdot \text{L}^{-1}$) or Cangrelor ($50 \mu\text{mol} \cdot \text{L}^{-1}$). $n = 3$ independent experiments, each condition in triplicate (B, C, D); $n = 4-7$ independent experiments for each condition (E). * $p < 0.05$, † $p < 0.01$, and ‡ $p < 0.001$ compared to the control without ADP or without APOA1 (PBS alone) or as indicated. NS indicates not significant ($p \geq 0.05$).

Figure 5: APOA1 mediates NO-dependent relaxation of human veins. Vessel rings were isolated from human umbilical veins (**A, C**) and placental veins (**B, D**). Pre-contraction of intact or endothelium-denuded vessels (w/o endoth.) was performed with U46619 ($100 \text{nmol} \cdot \text{L}^{-1}$), then vessels were exposed to APOA1 ($50 \mu\text{g} \cdot \text{mL}^{-1}$) or PBS (vehicle), in the presence of U46619, and changes in isometric tension were recorded for 20 min. L-NAME ($200 \mu\text{mol} \cdot \text{L}^{-1}$) or IF1 ($1.8 \mu\text{mol} \cdot \text{L}^{-1}$) was added to intact vessels 45 min before APOA1 treatment. $n = 3-6$ independent experiments for each condition. Bar graphs show the mean area under the curve (AUC) from 0 to 20 min. * $p < 0.05$, † $p < 0.01$, and ‡ $p < 0.001$ compared to the control with PBS alone or as indicated.

Figure 6: APOA1 increases NO-dependent blood flow in awake mice. **A**) Blood flow was measured in the femoral artery of mice infused for 45 min with different concentrations of APOA1. **B-C**) Blood flow was measured in the femoral artery of mice pre-infused for 30 min with PBS (vehicle), L-NMMA ($0.7 \mu\text{mol} \cdot \text{kg}^{-1} \cdot \text{min}^{-1}$) or IF1 ($60 \text{nmol} \cdot \text{kg}^{-1} \cdot \text{min}^{-1}$) and then co-infused for an additional 45 min with or without APOA1 ($30 \text{nmol} \cdot \text{kg}^{-1} \cdot \text{min}^{-1}$). Arrow indicates when the infusion of APOA1 began (at $t = 0$). $n = 3-4$ mice (A) and 6-9 mice (B, C) for each condition. Bar graphs represent the mean area under the curve (AUC) from 0 to 60 min. * $p < 0.05$, † $p < 0.01$, and ‡ $p < 0.001$ compared to the control with PBS alone or as indicated.

Figure 7: Changes in heart rate from baseline during infusions of vehicle or APOA1 in association or not with L-NMMA, IF1 or MRS2179. **A**) Heart rate was measured in mice pre-infused for 30 min with PBS (vehicle) and then co-infused for 45 min with different APOA1 concentrations. **B, C, D**) Heart rate was measured in mice pre-infused for 30 min with PBS (vehicle), L-NMMA ($0.7 \mu\text{mol} \cdot \text{kg}^{-1} \cdot \text{min}^{-1}$), IF1 ($60 \text{nmol} \cdot \text{kg}^{-1} \cdot \text{min}^{-1}$) or MRS2179 ($0.7 \mu\text{mol} \cdot \text{kg}^{-1} \cdot \text{min}^{-1}$) and then co-infused for an additional 45 min with or without APOA1 ($30 \text{nmol} \cdot \text{kg}^{-1} \cdot \text{min}^{-1}$). Arrow indicates when the infusion of APOA1 began (at $t = 0$). $n = 3-4$ mice (**A**) and 6-9 mice (**B, C, D**) for each condition. Bar graphs represent the mean area under the curve (AUC) of heart rate from 0 to 60 min. * $p < 0.05$ compared to the control with PBS alone.

Figure 8: ADP and APOA1 increase blood flow in awake mice through the activation of eNOS and the P2Y₁ receptor. **A-B**) Blood flow was measured in the femoral artery of mice pre-infused for 20 min with PBS (vehicle), L-NMMA ($1.5 \mu\text{mol} \cdot \text{kg}^{-1} \cdot \text{min}^{-1}$) or MRS2179 ($1.5 \mu\text{mol} \cdot \text{kg}^{-1} \cdot \text{min}^{-1}$) and then co-infused for an additional 20 min with or without 2meSADP ($0.7 \mu\text{mol} \cdot \text{kg}^{-1} \cdot \text{min}^{-1}$). **C**) Blood flow was measured in the femoral artery of mice pre-infused for 30 min with vehicle (PBS) or MRS2179 ($0.7 \mu\text{mol} \cdot \text{kg}^{-1} \cdot \text{min}^{-1}$) and then co-infused for an additional 45 min with or without APOA1 ($30 \text{nmol} \cdot \text{kg}^{-1} \cdot \text{min}^{-1}$). The arrow indicates when infusion of 2meSADP or APOA1 began (at $t = 0$). $n = 4-7$ mice for each condition. Bar graphs represent the mean area under the curve (AUC) from 0 to 60 min. Data with different superscript letters are significantly different. * $p < 0.05$ and ‡ $p < 0.001$ compared to the control with PBS alone.

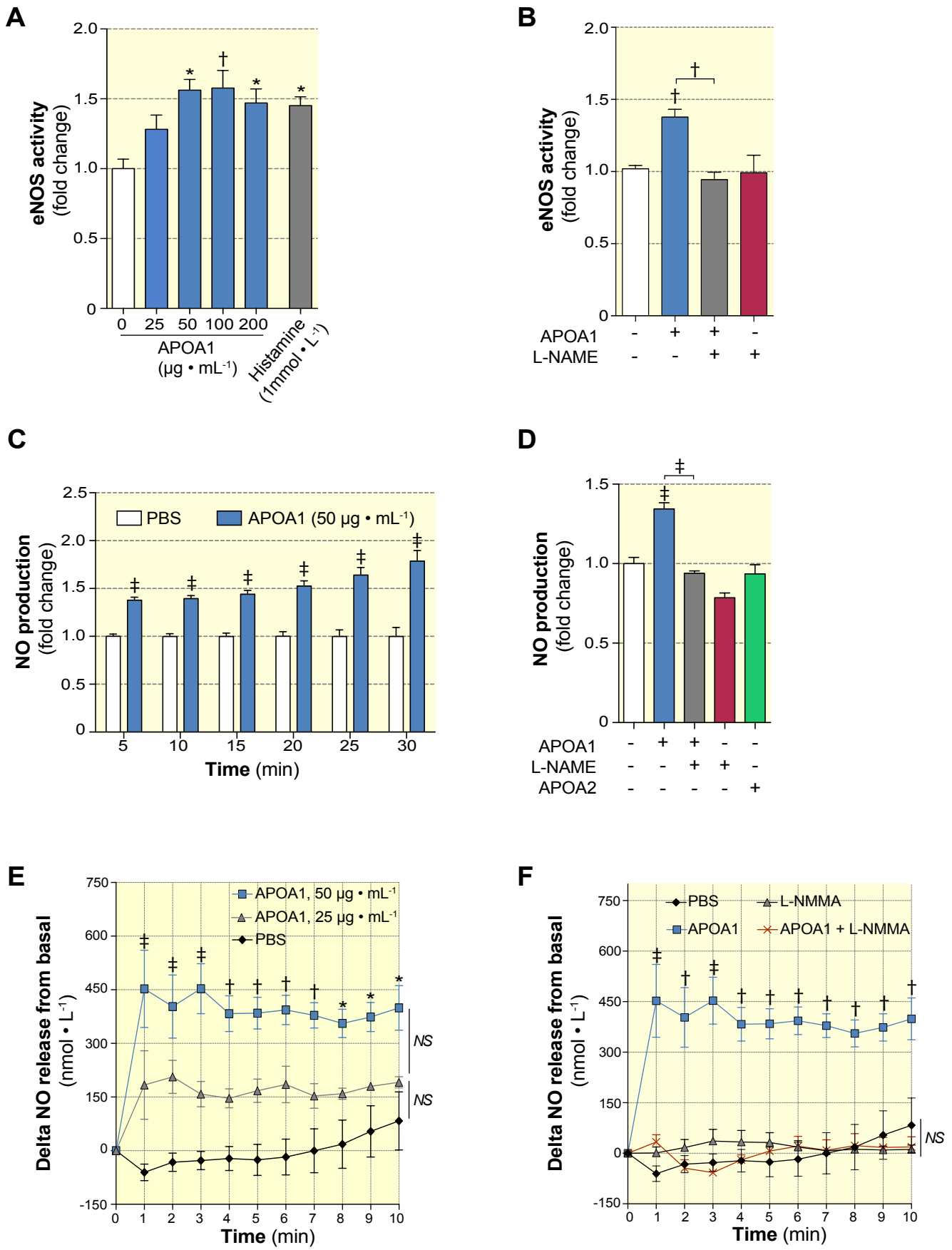
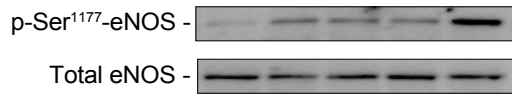
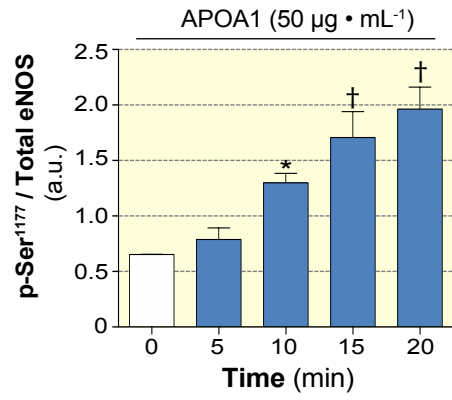
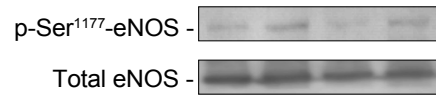
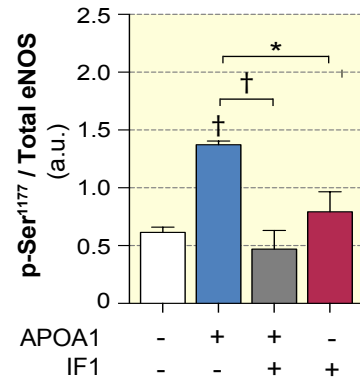
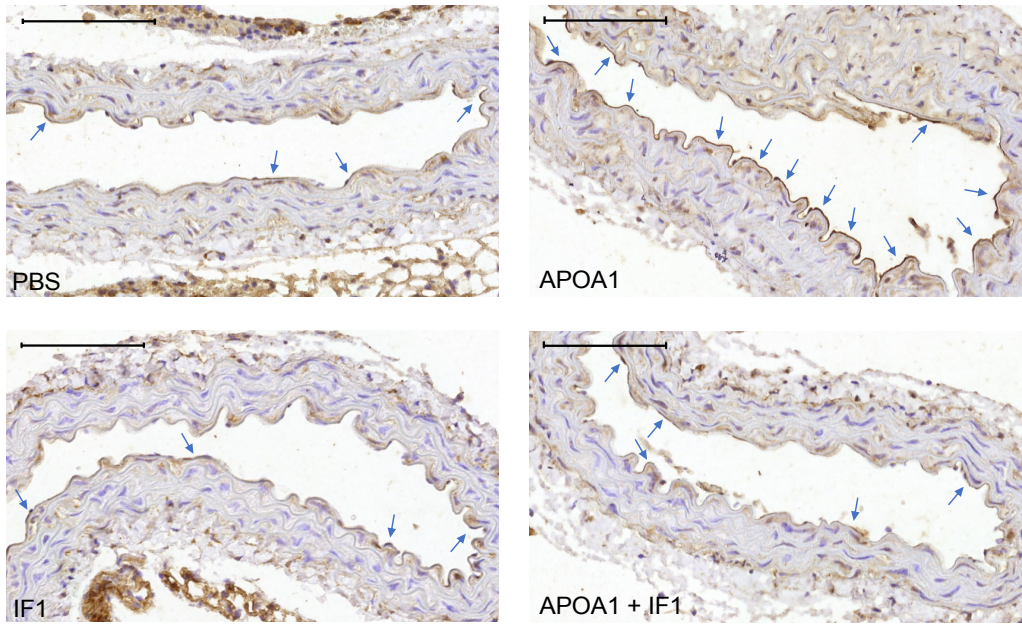
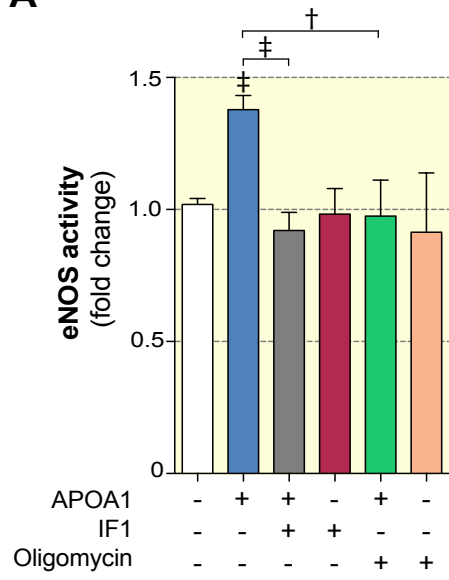
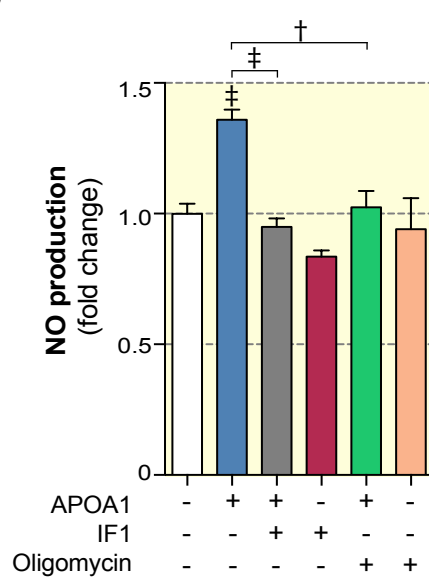
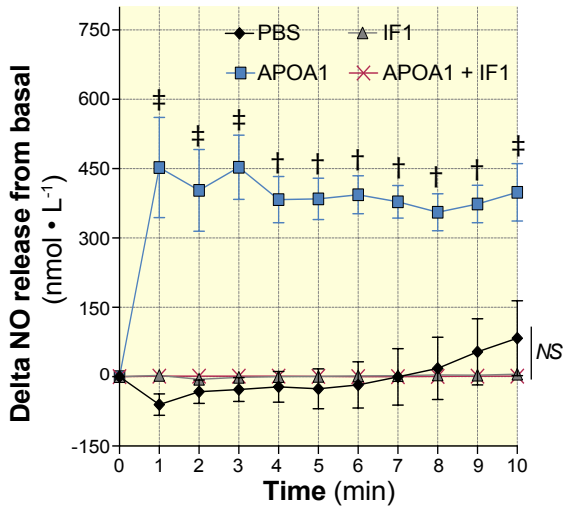
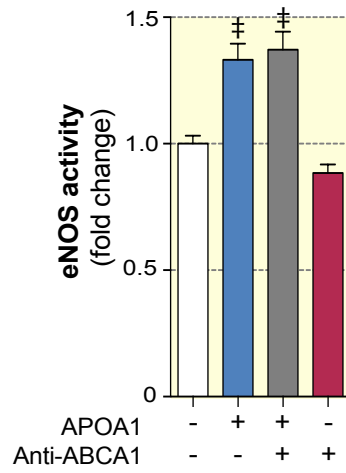
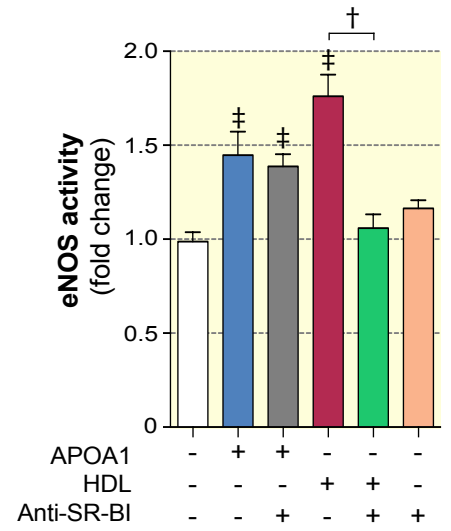


Figure 1

A**B****C****Figure 2**

A**B****C****D****E****Figure 3**

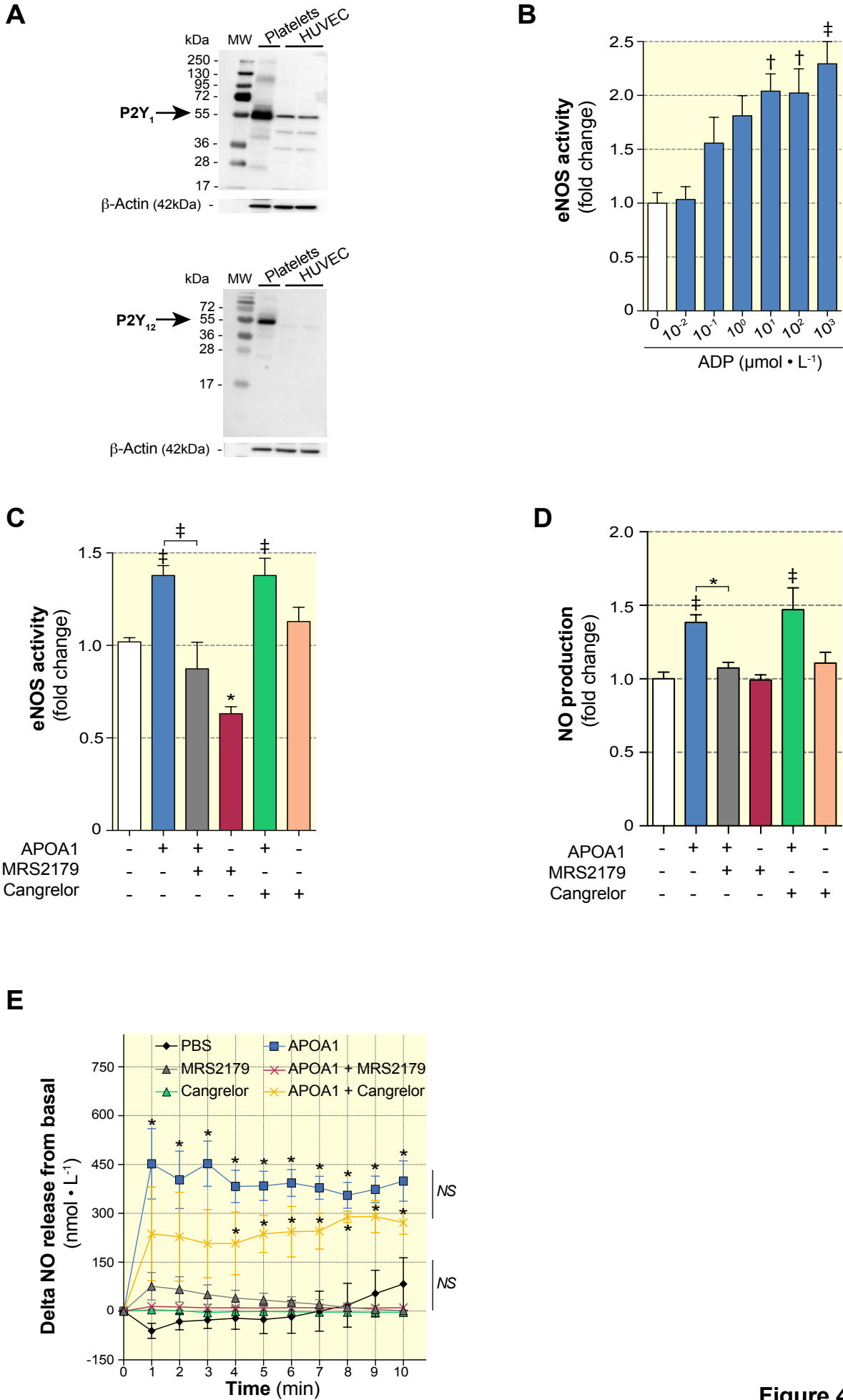
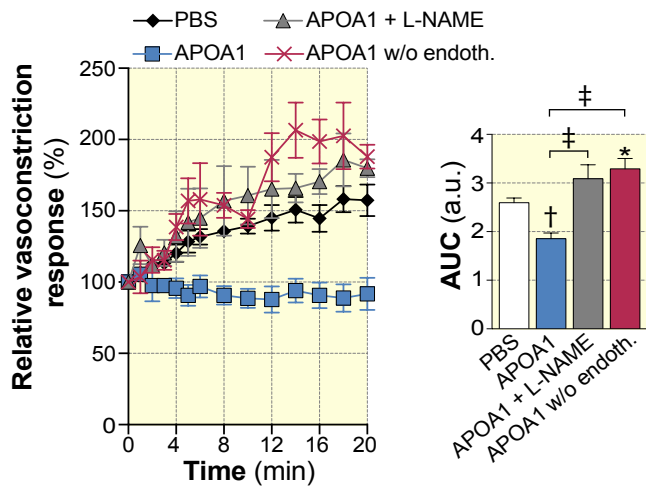
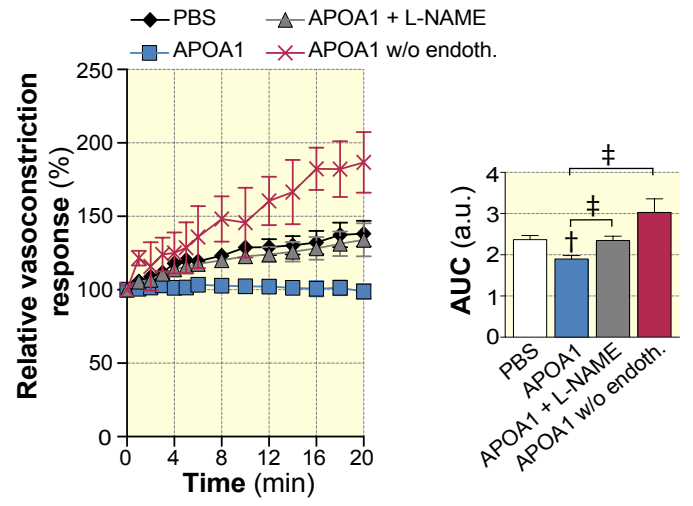
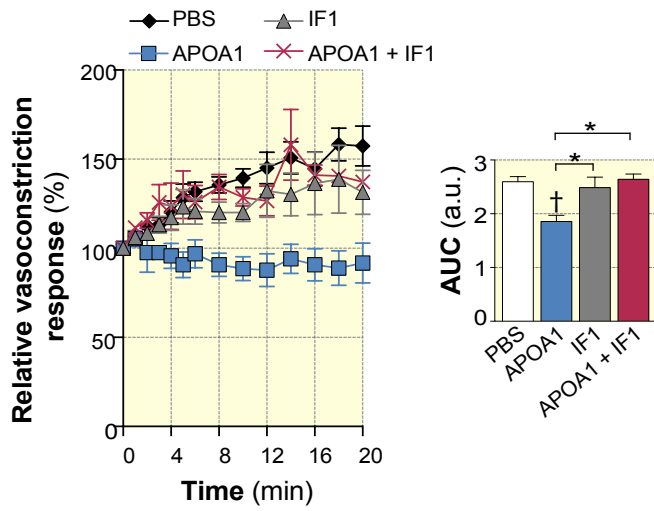
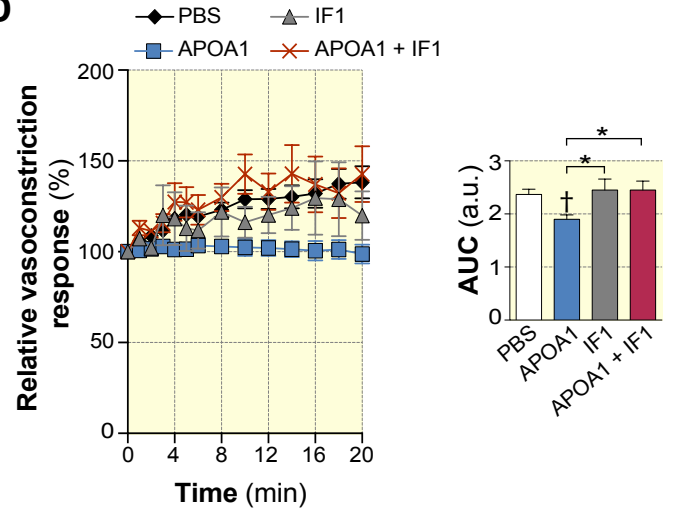
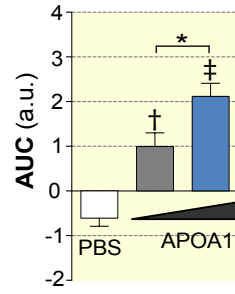
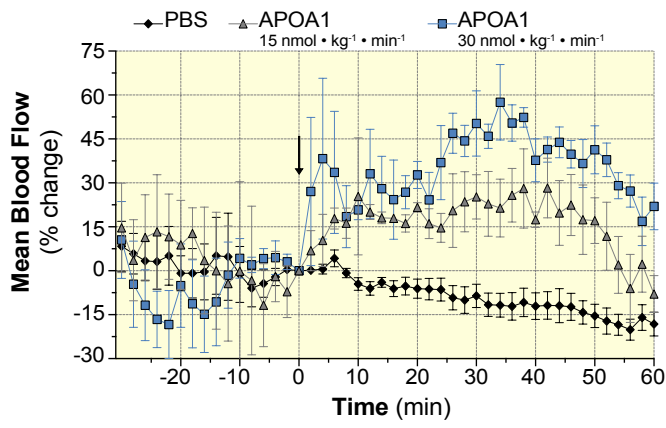
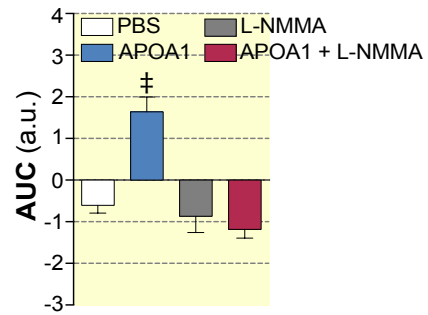
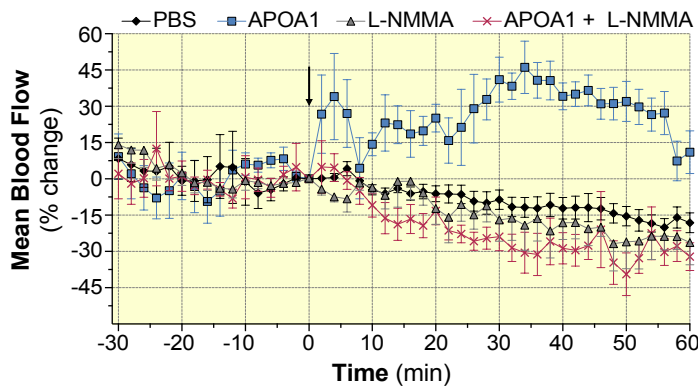
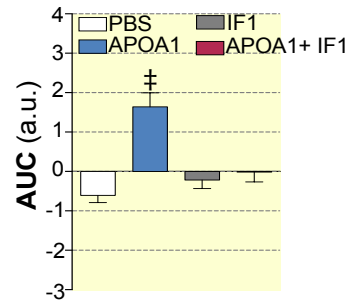
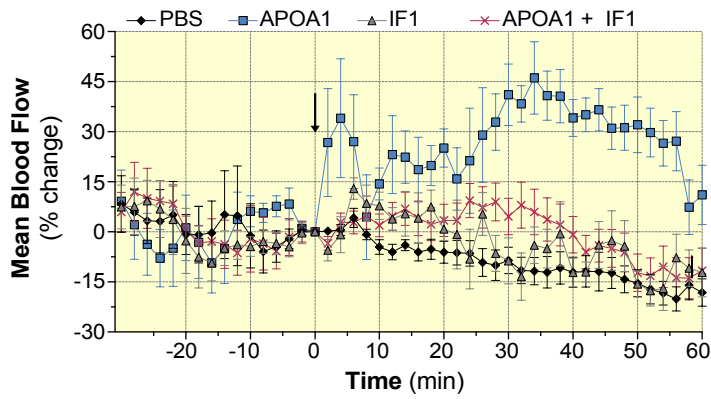


Figure 4

A**B****C****D****Figure 5**

A**B****C****Figure 6**

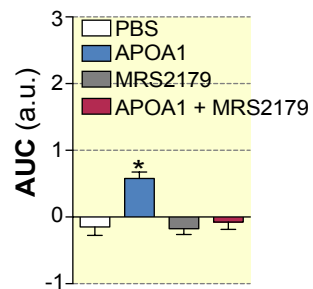
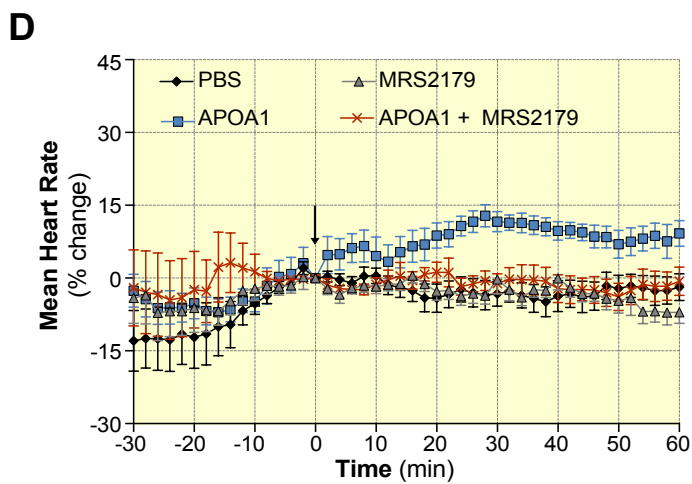
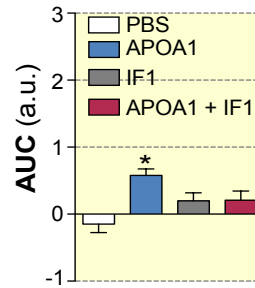
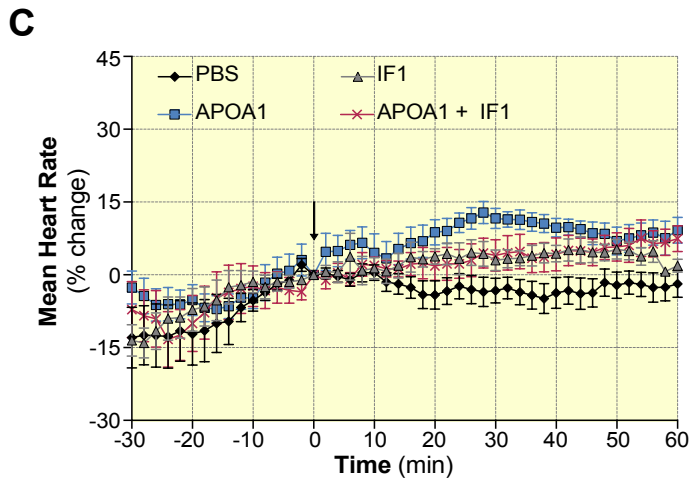
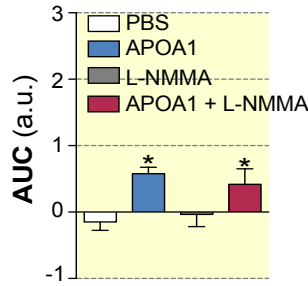
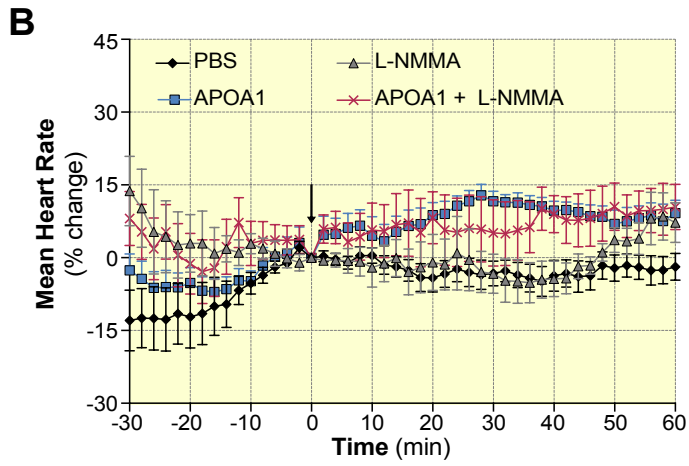
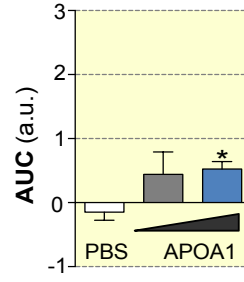
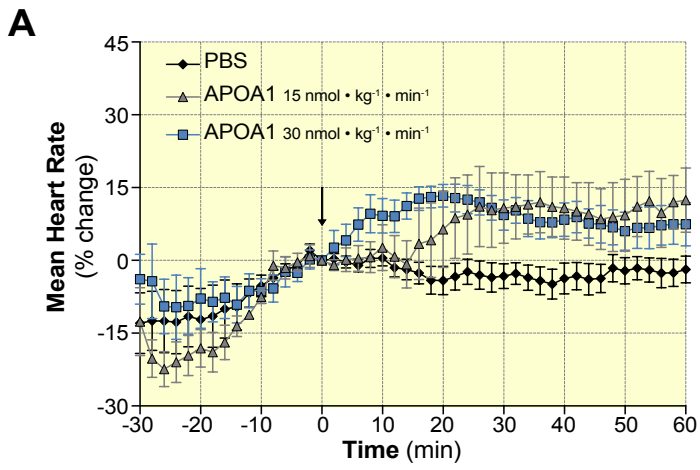
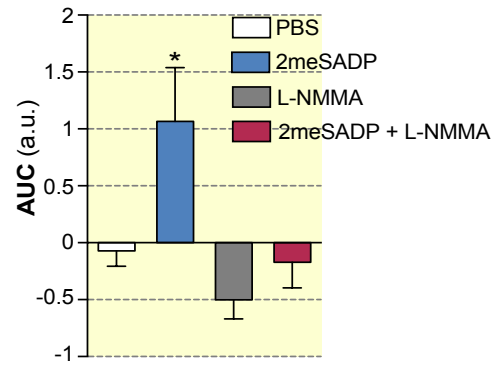
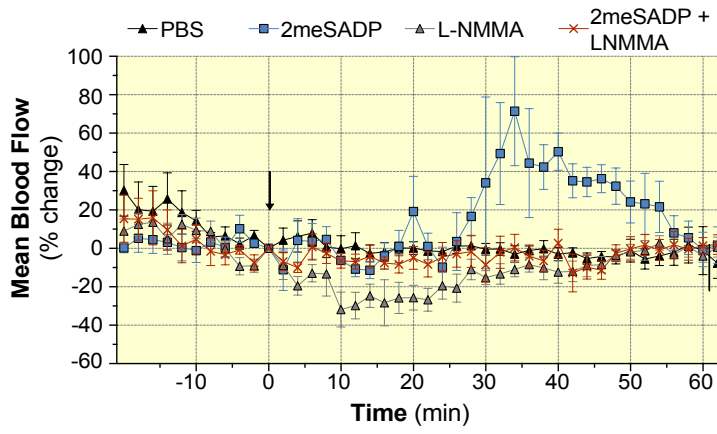
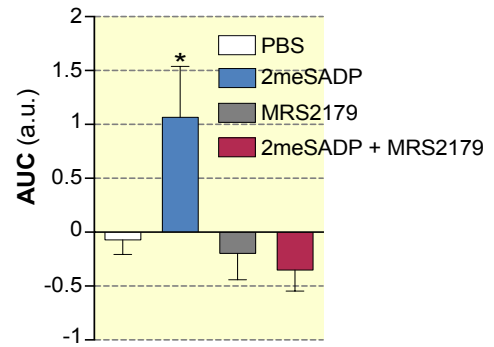
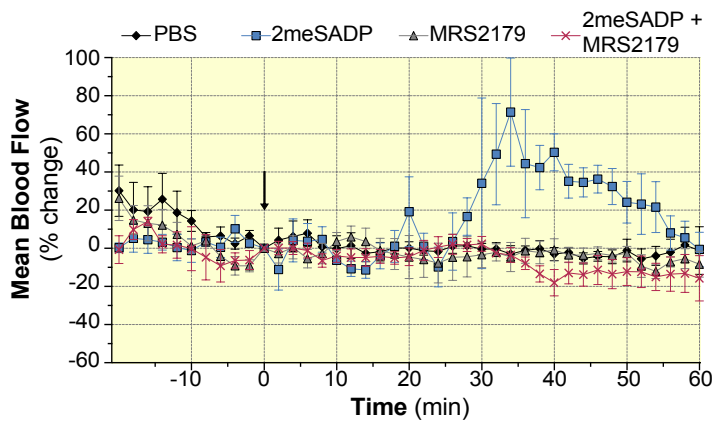
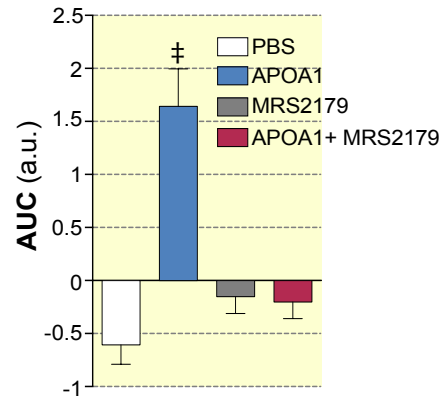
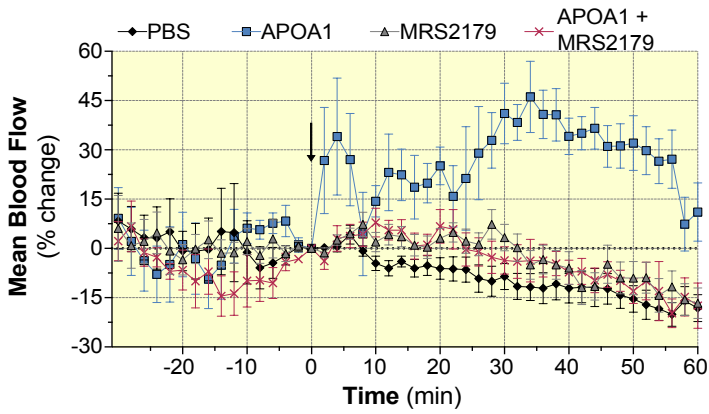


Figure 7

A**B****C****Figure 8**